Compléments pour le schéma explicite

Dans ce chapitre, nous présentons un calcul des coefficients de relaxation qui présente deux avantages sur celle présentée précédement. Le premier est qu'il permet de minimiser la diffusion numérique et le second est qu'il est plus simple et donc qu'il s'étend facilement aux systèmes compositionnels et triphasiques. Par ailleurs, nous détaillons la prise en compte des conditions aux limites.

4.1 Un autre calcul des coefficients de relaxation

Dans ce paragraphe, nous présentons une variante du calcul des coefficients de relaxation. Il doit être noté que, en effet, le développement de Chapman-Enskog ne donne qu'une indication sur la stabilité de la méthode : elle n'assure que la stabilité du problème quasi-linéaire associé. Nous allons vérifier qu'une approche différente permet de diminuer la diffusion numérique.

Par ailleurs, il doit être souligné que l'approche présentée dans l'article précédent est relativement complexe. En effet, si il est difficile d'assurer la positivité des valeurs propres d'une matrice d'ordre 3, il sera humainement impossible d'assurer la même condition pour une matrice d'ordre plus élevé. Or, comme nous allons le vérifier dans la deuxième partie de cette thèse, nous avons pour objectif final de traiter des système d'équations aux dérivées partielles de plus grande taille (par exemple le système à K constituants ou bien le système triphasique). Dans ce cadre, la méthode actuelle n'est plus envisageable et une alternative doit être trouvée.

Le plan de ce paragraphe est le suivant. Nous commençons par analyser la structure du système de relaxation en coordonnées Lagrangiennes. Puis nous faisons des liens entre le calcul des coefficients de relaxation actuels et des systèmes de lois de conservations plus simples (le p-système et une équation de conservation scalaire). Nous présentons alors la nouvelle manière de calculer les coefficients de relaxation. Cette nouvelle stratégie est soutenue par une expérience numérique spécialement choisie.

Reprenons le système d'équilibre gaz-liquide en coordonnées Eulériennes (2.16) avec $S = 0$:

$$\left\{ \begin{array}{ll} \partial_t \rho & + \partial_x(\rho v) = 0, \\ \partial_t(\rho v) & + \partial_x(\rho v^2 + P(\mathbf{u})) = 0, \\ \partial_t(\rho Y) & + \partial_x(\rho Y v - \sigma(\mathbf{u})) = 0. \end{array} \right. \tag{4.1}$$

4.1.1 Système relaxé en coordonnées Lagrangiennes

Afin de bien mettre en évidence les véritables non-linéarités du système, plaçons-nous en coordonnées Lagrangiennes. En introduisant le co-volume $\tau = \frac{1}{\rho}$ et la variable Lagrangienne y définie par

$$dx = vdt + \tau dy, \tag{4.2}$$

on aboutit à

$$\left\{\begin{array}{rcl} \partial_t\tau - \partial_y v &=& 0,\\ \partial_t v + \partial_y P &=& 0,\\ \partial_t Y - \partial_y \sigma &=& 0. \end{array}\right. \tag{4.3}$$

Par abus de notation, P et σ doivent être maintenant considérés comme des fonctions de (τ, v, Y).

On voit tout de suite que les difficultés théoriques sont concentrées dans P et σ, pression et impulsion apparentes. Ce sont par conséquent ces termes-là qu'il faut relaxer.

Remarque 4.1.1 *On considère ici le système (4.3). Introduisons une variable supplémentaire* Π *censée être égale à* P *et considèrons le système* 4×4 *suivant :*

$$\left\{\begin{array}{rcl} \partial_t\tau - \partial_y v &=& 0,\\ \partial_t v + \partial_y \Pi &=& 0,\\ \partial_t \Pi + a^2\,\partial_y v &=& \lambda\,(P-\Pi)\,,\\ \partial_t Y - \partial_y \sigma &=& 0. \end{array}\right. \tag{4.4}$$

La Jacobienne de ce système est

$$A = \begin{pmatrix} 0 & -1 & 0 & 0\\ 0 & 0 & 1 & 0\\ 0 & a^2 & 0 & 0\\ -\sigma_\tau & -\sigma_v & 0 & -\sigma_Y \end{pmatrix}. \tag{4.5}$$

Le système est hyperbolique et ses valeurs propres sont $(0,\ \pm a,\ -\sigma_Y)$*. La relaxation de l'équation de quantité de mouvement introduisant le coefficient a peut donc être vue comme un moyen de forcer l'hyperbolicité du système et d'assurer la positivité de la densité, comme nous allons le voir par la suite.*

Il apparaît par ailleurs que la dernière équation de (4.4) est non-linéaire. La relaxation de cette équation peut donc être vue comme un moyen de forcer la propriété physique $Y\in[0,1]$ *grâce au coefficient b, comme nous allons le voir par la suite.*

Introduisons une variable supplémentaire Σ, censée être égale à σ, et considérons le système 5×5 suivant :

$$\left\{\begin{array}{rcl} \partial_t\tau - \partial_y v &=& 0,\\ \partial_t v + \partial_y \Pi &=& 0,\\ \partial_t \Pi + a^2\,\partial_y v &=& \lambda\,(P-\Pi)\,,\\ \partial_t Y - \partial_y \Sigma &=& 0,\\ \partial_t \Sigma - b^2\,\partial_y Y &=& \lambda\,(\sigma-\Sigma)\,. \end{array}\right. \tag{4.6}$$

4.1.2 Calcul des coefficients de relaxation

Revenons en coordonnées eulériennes ; le système relaxé devient :

$$\partial_t \begin{pmatrix} \rho\\ \rho v\\ \rho\Pi\\ \rho Y\\ \rho\Sigma \end{pmatrix} + \partial_x \begin{pmatrix} \rho v\\ \rho v^2+\Pi\\ \rho\Pi v + a^2 v\\ \rho Y v - \Sigma\\ \rho\Sigma v - b^2 Y \end{pmatrix} = \begin{pmatrix} 0\\ 0\\ \lambda\rho\,(P-\Pi)\\ 0\\ \lambda\rho\,(\sigma-\Sigma) \end{pmatrix}. \tag{4.7}$$

Le système précédent s'écrit sous la forme abstraite

$$\partial_t \mathbf{v} + \partial_x \mathcal{G}(\mathbf{v}) = \lambda \mathcal{R}(\mathbf{v}) \tag{4.8}$$

où les définitions sont évidentes.

On cherche à s'assurer de la stabilité du problème relaxé et du caractère stable de la méthode. Plus concrètement, on souhaite pouvoir énoncer des conditions suffisantes pour que le système soit dissipatif. Comme le problème de Tacite ne possède pas de propriété d'entropie qu'on peut habituellement désirer dans le contexte hyperbolique, on va se contenter de traiter la question de façon locale, par développement asymptotique vis-à-vis de λ.

4.1.2.1 Ancienne technique de calcul des coefficients de relaxation

Dans ce paragraphe, nous présentons la technique initialement envisagée pour le calcul des coefficients de relaxation ainsi que les raisons qui nous ont fait abandonner cette technique. Dans cette technique, le système de relaxation était réduit par le développement de Chapman-Enskog à la forme quasi-linéaire :

$$\partial_t \mathbf{w} + \Gamma(\mathbf{w}) \partial_y \mathbf{w} = \lambda^{-1} \partial_y \left[\Delta(\mathbf{w}) \partial_y \mathbf{w} \right], \tag{4.9}$$

avec $\mathbf{w} = (\tau,\, v,\, \Pi,\, Y,\, \Sigma)^T$ et Γ la Jacobienne du système d'équilibre en coordonnées Lagrangiennes. Nous assurions la positivité des valeurs propres de la matrice de diffusion $\Delta_{a,b}(\mathbf{w})$

$$\Delta_{a,b}(\mathbf{w}) = \begin{pmatrix} 0 & 0 & 0 \\ E & a^2 - A & C \\ F & D & b^2 - B \end{pmatrix} \tag{4.10}$$

avec comme coefficients

$$\begin{array}{ll} E = -P_v P_\tau + P_Y \sigma_\tau, & F = \sigma_v P_\tau - \sigma_Y \sigma_\tau, \\ A = \underline{-P_\tau + P_v^2} - P_Y \sigma_v, & D = -\sigma_\tau + \sigma_v P_v - \sigma_Y \sigma_v, \\ C = -P_v P_Y + P_Y \sigma_Y, & B = \underline{\sigma_Y^2} - \sigma_v P_Y. \end{array}$$

Nous voudrions ici mettre en lumière la structure très singulière de ces coefficients.

Le coefficient $-P_\tau + P_v^2$ dans A est un terme intrinsèquement lié au sous-système `(A)` : il contient les dérivées de P par rapport aux variables d'équilibre régies par les équations d'évolution de ce sous-système, c'est-à-dire τ et v.

Le coefficient σ_Y^2 dans B est un terme intrinsèquement lié au sous-système `(B)` : il contient la dérivée de σ par rapport à la seule variable d'équilibre régie par une équation d'évolution dans ce sous-système, c'est-à-dire Y.

Tous les autres termes sont en fait des termes de couplages entre sous-systèmes. Notons par ailleurs que l'étude (en annexe) du système de relaxation avec glissement nul produit un coefficient $A = -p_\tau$. D'autre part, si l'équation d'évolution en Y était une simple équation scalaire, découplée des autres variables, le coefficient sortant du calcul serait $B = \sigma_Y^2$.

D'un tout autre point de vue, certains cas-tests exhibent des coefficients a et b tout à fait surestimés, lorsqu'on considère l'approche du rapport antérieur. Cela se traduit par une diffusion trop importante. Un cas-test de ce type est présenté à la fin de ce chapitre.

C'est cet ensemble de remarques qui nous a conduit à formuler le développement de Chapman-Enskog suivant.

4.1.2.2 Nouvelle technique de calcul des coefficients de relaxation

Nous allons considérer le développement de Chapman-Enskog de chaque sous-système en supposant qu'ils sont découplés. Soulignons que cette stratégie est une heuristique et que le développement de Chapman-Enskog est un calcul qui n'assure la stabilité du système de relaxation que de manière formelle. Ces justifications seront reprises dans l'article du chapitre suivant [7].

4.1.2.2.1 Sous-système relaxé 1 en Lagrangien Considérons le premier sous-système :

$$\left\{ \begin{array}{rcl} \partial_t \tau - \partial_y v &=& 0, \\ \partial_t v + \partial_y \Pi &=& 0, \\ \partial_t \Pi + a^2 \partial_y v &=& \lambda(P - \Pi). \end{array} \right. \tag{4.11}$$

Le développement de Chapman-Enskog pour ce sous-système est par définition :

$$\Pi = P + \lambda^{-1}\Pi_1 + \mathcal{O}(\lambda^{-2}). \tag{4.12}$$

Nous faisons alors l'hypothèse suivante. *La fonction P dépend uniquement de τ et v* de telle sorte que :

$$P = P(\tau, v). \tag{4.13}$$

On peut alors mettre le sous-système sous la forme *quasi-linéaire* avec $\mathbf{w}^1 = (\tau, v)^T$:

$$\partial_t \mathbf{w}^1 + \Gamma^1(\mathbf{w}^1)\partial_y \mathbf{w}^1 = \lambda^{-1}\partial_y \left[\Delta_a(\mathbf{w}^1)\partial_y \mathbf{w}^1\right], \tag{4.14}$$

$$\Delta_a(\mathbf{w}^1) = \begin{pmatrix} 0 & 0 \\ E & a^2 - A \end{pmatrix}, \quad E = -P_v P_\tau, \quad A = -P_\tau + P_v^2. \tag{4.15}$$

La matrice $\Delta_a(\mathbf{w}^1)$ a des valeurs propres positives si et seulement si

$$a^2 - A \geq 0, \tag{4.16}$$

condition qui assure la stabilité du premier sous-système.

4.1.2.2.2 Sous-système relaxé 2 en Lagrangien Considérons le second sous-système :

$$\left\{ \begin{array}{rcl} \partial_t Y - \partial_y \Sigma &=& 0, \\ \partial_t \Sigma - b^2 \partial_y Y &=& \lambda(\sigma - \Sigma). \end{array} \right. \tag{4.17}$$

Le développement de Chapman-Enskog pour ce sous-système est par définition :

$$\Sigma = \sigma + \lambda^{-1}\Sigma_1 + \mathcal{O}(\lambda^{-2}). \tag{4.18}$$

Nous faisons alors l'hypothèse suivante. *La fonction σ dépend uniquement de Y* de telle sorte que :

$$\sigma = \sigma(Y). \tag{4.19}$$

On peut alors mettre le sous-système sous la forme *quasi-linéaire* :

$$\partial_t Y - \partial_y \sigma = \lambda^{-1}\partial_y \left[\Delta_b(Y)\partial_y Y\right], \tag{4.20}$$

$$\Delta_b(Y) = b^2 - B, \quad B = \sigma_Y^2. \tag{4.21}$$

Le coefficient $\Delta_b(Y)$ est positif si et seulement si

$$b^2 - B \geq 0, \tag{4.22}$$

condition qui assure la stabilité du second sous-système.

Lorsque $\varphi = 0$, $B = 0$ donc $b = 0$. Comme c'est incompatible avec la méthode (solveur de Riemann, Matrice de Roe, ...), on prend :

$$b^2 = \max(B, 1). \tag{4.23}$$

Le coefficient 1 de l'équation précédente a été choisit car, dans le cas d'un glissement non nul, le coefficient b prend généralement des valeurs entre quelques centaines et plusieurs milliers. Nous avons donc considéré que 1 était petit devant ces nombres et qu'il n'augmentait pas la diffusion numérique de façon significative.

Remarque 4.1.2 *Compte tenu des valeurs des dérivées respectives de P et σ, on a toujours :*

$$a > b. \tag{4.24}$$

C'est bien cohérent avec le fait que a relaxe des ondes de pression et b des ondes de transport de masse.

4.1.3 Nouveau calcul pratique des coefficients de relaxation

Nous considérons un couple de coefficient (a, b) par arête et les développements précédents justifient que l'on prenne :

$$a_{i+1/2} = \sqrt{\max(A(\mathbf{u_L}), A(\mathbf{u_R}))}, \qquad b_{i+1/2} = \sqrt{\max(B(\mathbf{u_L}), B(\mathbf{u_R}))}, \tag{4.25}$$

$$A(\mathbf{u}) = -P_\tau(\mathbf{u}) + P_v^2(\mathbf{u}), \qquad B(\mathbf{u}) = \sigma_Y^2(\mathbf{u}). \tag{4.26}$$

Cette stratégie de coefficients de relaxation locaux (par arête) permet d'obtenir la diffusion minimale.

4.1.4 Expérience numérique

Dans ce paragraphe, nous présentons une expérience numérique qui montre l'intérêt de l'approche découplée dans le développement de Chapman-Enskog, approche qui mène à un nouveau calcul des coefficients de relaxation. Nous allons vérifier que cette approche permet de diminuer de façon importante la diffusion numérique.

Considérons les deux états

$$\begin{pmatrix} \rho \\ Y \\ v \end{pmatrix}_{\mathbf{L}} = \begin{pmatrix} 901.111 \\ 1.2330.10^{-3} \\ 0.70316 \end{pmatrix} \qquad \text{et} \qquad \begin{pmatrix} \rho \\ Y \\ v \end{pmatrix}_{\mathbf{R}} = \begin{pmatrix} 208.886 \\ 4.2541.10^{-2} \\ -0.28052 \end{pmatrix}$$

Les autres paramètres sont : $a_{\mathrm{G}} = 300$ m/s, $c_0 = 1.07$, $c_1 = 0.2162$ m/s. On utilise dans ce cas 50 mailles, comme dans les cas réels. La solution est une Discontinuité de Contact qui se propage à la vitesse $v_{\mathrm{G}} = 1$ m/s. Les instantanés de la figure (4.1) correspondent au temps $T = 20.$ s avec un schéma d'ordre 1 en espace et en temps.

Cette expérience permet de tester le schéma avec un grand nombre d'itérations car la discontinuité de contact se propage à une vitesse lente. C'est donc une expérience relativement proche des cas réels, dans lesquels les ondes se déplacent à des vitesses lentes. C'est également une expérience qui met les schémas à l'épreuve car la diffusion, à cause du grand nombre d'itérations, est importante.

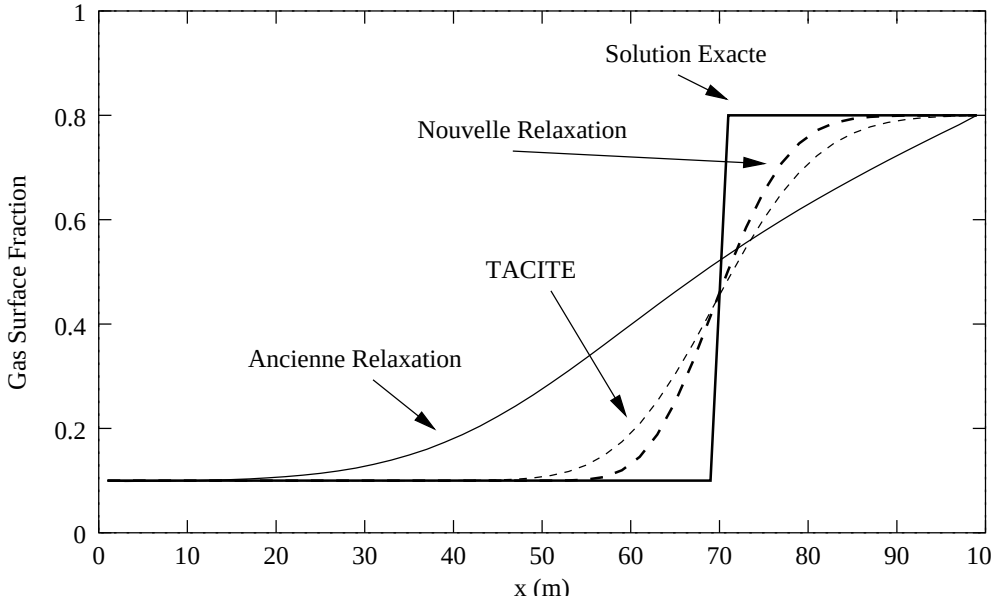

FIG. 4.1 – Discontinuité de contact pour le modèle de Zuber-Findlay.

On compare dans cette expérience le schéma de Relaxation avec les coefficients de Relaxation calculés par la méthode présentée dans le précédent rapport ("Ancienne Relaxation ") avec la méthode (dite "Nouvelle Relaxation ") présentée dans ce rapport. On constate que la nouvelle est bien meilleure, grâce à une diffusion bien plus faible. On obtient des résultats comparables au schéma TACITE , même un peu meilleurs.

Dans le but de comprendre une différence de comportement aussi importante, examinons les coefficients de Relaxation dans les deux cas. A la première itération en temps, les coefficients de Relaxation avec la technique initiale sont :

$$(a,b)^1_{\mathbf{L}} = (95408., 8578.), \quad (a,b)^1_{\mathbf{R}} = (18887., 9721.) \tag{4.27}$$

et avec la nouvelle :

$$(a,b)^2_{\mathbf{L}} = (94926., 267.), \quad (a,b)^2_{\mathbf{R}} = (16156., 279.) \tag{4.28}$$

On comprend bien alors comment cette large sur-estimation du coefficient b conduit à une diffusion très importante sur cette discontinuité de contact. Les effets de cette sur-estimation ne se font sentir que dans le cas de la conduite verticale, présenté plus loin, avec le schéma semi-implicite linéaire.

4.2 Traitement aux limites

Nous présentons ici la technique utilisée pour calculer les points fictifs amont et aval.

Le traitement des conditions aux limites est à la fois essentiel et extrêment délicat. C'est un problème peu connu d'un point de vue théorique (pour les systèmes d'équations aux dérivées partielle) et difficile d'un point de vue numérique dans le cadre des écoulements en conduite. Plus spécifiquement, comme toutes les informations qui entrent dans la conduite pétrolière entrent par l'amont, le traitement de la condition limite amont est très important. Autrement dit, il est inutile de construire un schéma numérique intérieur précis si la condition à la limite amont n'est pas traitée de façon adéquate.

Or, il y a une difficulté à prendre en compte les conditions aux limites lorsqu'on considère un schéma semi-implicite. En effet, lorsqu'on considère un schéma explicite, une stratégie qui consiste à contrôler la solution du problème de Riemann sur l'arête limite est suffisante (c'était notre premier choix, voir [10]). En fait, si on utilise un schéma explicite, une méthode qui se contente de fournir le flux numérique sur l'arête limite (comme dans [27]) fonctionne bien.

Mais dans le cadre d'un schéma semi-implicite, dans la phase mathématique du schéma, les états fictifs $\mathbf{u}_0 = (\rho_0,\ \rho_0 Y_0,\ \rho_0 v_0)$ et $\mathbf{u}_{I+1} = (\rho_{I+1},\ \rho_{I+1}Y_{I+1},\ \rho_{I+1}v_{I+1})$ sont utilisés dans le calcul des matrices de diffusion $A^{Roe}(\mathbf{u}_0,\ \mathbf{u}_1)$ et $A^{Roe}(\mathbf{u}_I,\ \mathbf{u}_{I+1})$. Ainsi, notre schéma semi-implicite nous oblige à connaitre explicitement les états fictifs, ce qui n'est pas sans poser de problèmes.

Nous décidons de nous inspirer, pour la prise en compte des conditions aux limites, de la stratégie qui a fonctionné pour le schéma Tacite. Cette stratégie est globalement fondée sur le signe des valeurs propres. De plus, nous imposons que les variables de relaxation correspondant aux états fictifs doivent être à l'équilibre.

Nous allons voir que, concernant la prise en compte de la condition limite amont, la méthode implique que l'état fictif amont est solution d'un problème non-linéaire, ce qui oblige à utiliser une méthode de résolution approchée (par exemple une méthode de Newton). A l'heure actuelle, il n'existe pas de théorème d'existence de l'état fictif amont dans le cadre des écoulements diphasiques et la méthode de Newton n'est pas garantie de converger.

En ce qui concerne la condition limite aval, nous imposons une condition dite de "non-retour de liquide" qui n'est pas usuelle. Cette condition, difficile à prendre en compte numériquement, est le sujet de résultats théoriques présentés par Gallouët dans [29] et qui sont l'application de résultats dûs à Vovelle [62]. Ils montrent en particulier que la stratégie utilisée ici fonctionne correctement, en particulier parceque la fonction flux numérique reste continue en fonction de l'état fictif.

4.2.1 Amont

À l'entrée de la conduite, les conditions aux limites physique sont le débit de liquide q_{L} et le débit de gaz q_{G}. En pratique, les débits q_{L} et q_{G} sont donnés en fonction du temps t.

On connaît l'état sur la première maille $\mathbf{v}_1^n$ et on cherche l'état gauche fictif $\mathbf{v}_0^n$ de la façon suivante.

Rappelons que $\mathbf{v}_0^n$ possède 5 composantes :

$$\mathbf{v}_0^n = (\rho_0^n,\ q_0^n,\ \chi_0^n,\ I_0^n,\ J_0^n)$$

où l'on note $q_0^n = (\rho v)_0^n$, $\chi_0^n = (\rho Y)_0^n$, $I_0^n = (\rho\Pi)_0^n$, $J_0^n = (\rho\Sigma)_0^n$. Le flux numérique sur la première arête est une fonction des deux états $\mathbf{v}_0^n$ et $\mathbf{v}_1^n$:

$$\mathbf{H}_{1/2} = \mathbf{H}(\mathbf{v}_0^n,\ \mathbf{v}_1^n) \tag{4.29}$$

Notons $\{h_i\}_{i=1,5}$, les cinq composantes du flux $\mathbf{H}_{1/2}$. La première composante h_1 est le débit total, somme du débit de gaz et du débit de liquide à t^n. La quatrième composante h_4 est le débit de gaz à $t = t^{n+1/2}$. On impose le débit total, le débit de gaz ainsi que l'équilibre des variables de relaxation :

$$h_1(\mathbf{v}_0^n,\ \mathbf{v}_1^n) = q_{\mathrm{L}} + q_{\mathrm{G}}, \qquad h_4(\mathbf{v}_0^n,\ \mathbf{v}_1^n) = q_{\mathrm{G}}, \tag{4.30}$$

$$I_0^n = \rho_0^n P(\rho_0^n,\ q_0^n,\ \chi_0^n), \quad J_0^n = \rho_0^n \sigma(\rho_0^n,\ q_0^n,\ \chi_0^n). \tag{4.31}$$

Cependant, cela ne fait que 4 équations, alors qu'il y a 5 composantes inconnues pour $\mathbf{v}_0^n$. Pour déterminer complètement $\mathbf{v}_0^n$, on traduit la propagation de droite à gauche correspondant à l'onde sortante λ_1 en utilisant la projection caractéristique :

$$(\ell|\mathbf{v}_0^n) = (\ell|\mathbf{v}_1^n), \tag{4.32}$$

où $\ell = \ell(\mathbf{v}_0^n,\ \mathbf{v}_1^n)$ est le vecteur propre à gauche associé à la première valeur propre λ_1 de la matrice Jacobienne du système de relaxation sur la première maille $\nabla\mathcal{G}(\mathbf{v}_1^n)$.

Notons α la fonction :

$$\alpha(\mathbf{v}_0^n, \mathbf{v}_1^n) = (\ell|\mathbf{v}_0^n) - (\ell|\mathbf{v}_1^n)$$

L'état fictif amont $\mathbf{v}_0^n$ est solution du système non linéaire :

$$\mathbf{F}(\mathbf{v}_0^n) = \begin{pmatrix} h_1(\mathbf{v}_0^n,\ \mathbf{v}_1^n) - (q_\mathrm{L} + q_\mathrm{G}) \\ h_3(\mathbf{v}_0^n,\ \mathbf{v}_1^n) - q_\mathrm{G} \\ \alpha(\mathbf{v}_0^n,\ \mathbf{v}_1^n) \\ I_0^n - \rho_0^n P(\rho_0^n,\ \chi_0^n,\ q_0^n) \\ J_0^n - \rho_0^n \sigma(\rho_0^n,\ \chi_0^n,\ q_0^n) \end{pmatrix} = 0 \tag{4.33}$$

Notons désormais $\mathbf{x} = \mathbf{v}_0^n$ la solution de ce système. La résolution est fondée sur une méthode de Newton : on initialise $\mathbf{x}^0$ de façon adaptée puis on calcule $\Delta\mathbf{x}^k$ et $\mathbf{x}^{k+1}$ tels que :

$$\nabla\mathbf{F}(\mathbf{x}^k)\Delta\mathbf{x}^k = -\mathbf{F}(\mathbf{x}^k), \qquad \mathbf{x}^{k+1} = \mathbf{x}^k + \Delta\mathbf{x}^k.$$

Remarque 4.2.1 *La stratégie consistant à utiliser une projection caractéristique est fondée sur le signe des valeurs propres du système d'équilibre. En effet, la première valeur propre λ_1, associée aux ondes acoustiques, est toujours négative. C'est par conséquent la projection caractéristique sur le premier champ qui contient l'information sortant du domaine.*

Rappelons que cette projection est issue du fait suivant. Soit le système d'EDP linéaire :

$$\partial_t\mathbf{u} + \nabla\mathcal{F}\,\partial_x\mathbf{u} = 0, \tag{4.34}$$

avec $\mathbf{u} \in \mathbb{R}^N$ et $\nabla\mathcal{F}$ une matrice d'ordre N à coefficients constants. Supposons que ℓ est un vecteur vecteur propre à gauche de $\nabla\mathcal{F}$ tel que : $\ell\mathcal{F} = \lambda_1\ell$. Comme le système est à coefficients constants, nous avons $\partial_t\ell = 0$ et $\partial_x\ell = 0$. Par conséquent, en faisant le produit scalaire de (4.34) par ℓ, on obtient :

$$\partial_t(\ell|\mathbf{u}) + \lambda_1\,\partial_x(\ell|\mathbf{u}) = 0$$

c'est à dire que $(\ell|\mathbf{u})$ est un invariant de Riemann fort pour la valeur propre λ_1.

Cette propriété n'est, pour un système non-linéaire comme le nôtre, qu'une approximation, puisque nous n'avons pas $\partial_t\ell = 0$, $\partial_x\ell = 0$. Pourtant, il s'avère qu'en pratique cette technique fonctionne de façon satisfaisante. En particulier, c'est la stratégie adoptée dans le code Tacite.

4.2.2 Aval

À l'aval, on impose la pression p_{I+1} comme condition physique sur la maille fictive $I+1$.

Cela ne fait qu'une condition scalaire pour les 5 inconnues de la variable de relaxation $\mathbf{v}_{I+1}^n$. De même qu'à l'amont, nous imposons l'équilibre des variables de relaxation ce qui fait 2 équations. Enfin, nous aurions pu considérer 2 projections caractéristiques menant à la résolution d'un système non-linéaire. L'expérience pourtant montre qu'il suffit d'imposer

$$Y_{I+1}^n = Y_I^n, \quad v_{I+1}^n = v_I^n. \tag{4.35}$$

En pratique, connaissant la pression, on peut, grâce aux lois thermodynamiques calculer $\rho_\mathrm{L} = \rho_\mathrm{L}(p_{I+1})$ et $\rho_\mathrm{G} = \rho_\mathrm{G}(p_{I+1})$ puis la masse volumique sur la dernière maille par

$$\rho_{I+1}^n = \frac{1}{\frac{1-Y_I}{\rho_\mathrm{L}} + \frac{Y_I}{\rho_\mathrm{G}}}. \tag{4.36}$$

Ceci nous permet alors de définir entièrement l'état fictif aval et donc de calculer le flux numérique sur la dernière arête $\widetilde{\mathbf{H}}_{I+1/2}$, dont on allons voir que, pour obtenir le flux définitif, nous modifions certaines composantes.

En effet, sur le terrain, un système appelé *séparateur* (voir figure 4.2) a pour but d'empêcher le retour du liquide dans la conduite. En termes mathématiques, cela revient à exiger que le débit de liquide q_{L} reste positif à l'aval. C'est pourquoi, après avoir calculé le flux aval $\widetilde{\mathbf{H}}_{I+1/2}$, on considère $q_{\mathrm{L}} = \widetilde{h}_1 - \widetilde{h}_3$ et $q_{\mathrm{G}} = \widetilde{h}_3$. Si $q_{\mathrm{L}} < 0$, on impose $q_{\mathrm{L}} = 0$ et on recalcule $h_1 = q_{\mathrm{G}}$. Ainsi le flux numérique définitif est $\mathbf{H}_{I+1/2} = (h_1, \widetilde{h}_2, \widetilde{h}_3, \widetilde{h}_4, \widetilde{h}_5)^T$ avec

$$h_1 = \begin{cases} \widetilde{h}_3, \text{ si } \widetilde{h}_1 - \widetilde{h}_3 < 0, \\ \widetilde{h}_1, \text{ sinon.} \end{cases} \tag{4.37}$$

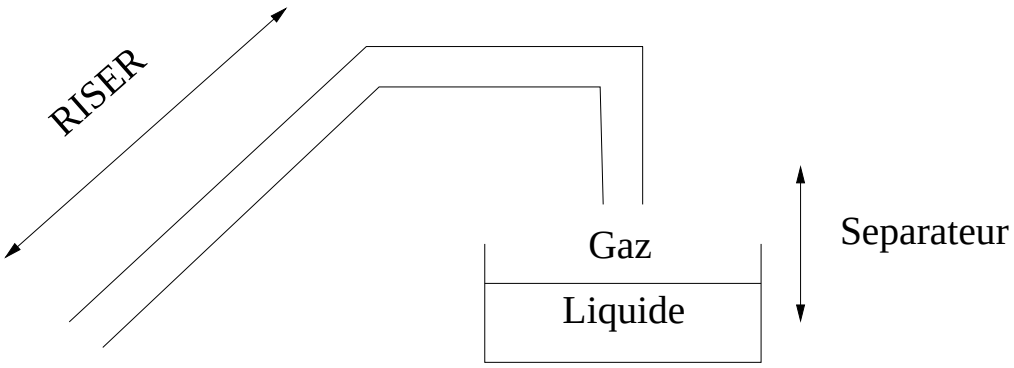

FIG. 4.2 – Riser se déversant dans un séparateur

Chapitre 5

A semi-implicit relaxation scheme for modeling two-phase flow in a pipeline

Michaël BAUDIN[1], **Frédéric COQUEL**[2] **and Quang Huy TRAN**[1]

[1] IFP, 1 et 4 avenue de Bois-Préau, 92852 Rueil-Malmaison Cedex, France
[2] Lab. J.-L. Lions, Université Pierre et Marie Curie, Boîte courrier 187, 75252 Paris Cedex 5

Abstract This work is devoted to the numerical approximation of the solutions of the system of conservation laws which arises in the modeling of two-phase flows in oil and gas pipeline. The PDEs are closed by two highly nonlinear algebraic relations, namely : a pressure law and a hydrodynamic law. We have previously developed an explicit relaxation scheme which allows to cope with these nonlinearities. But the system considered has eigenvalues which are of very different orders of magnitude, which prevents the explicit scheme from being effective, since the time-step has to be very small. In order to solve this effectiveness problem, we now proceed to construct a scheme which is explicit with respect to the small eigenvalues and linearly implicit with respect to the large eigenvalues. Numerical evidences are proposed.

Key words two-phase flows, relaxation scheme, semi-implicit, Riemann solvers
AMS subject classification 76T10, 76N15, 35L65, 65M06

Introduction

We are interested in the simulation of two-phase flows in petroleum pipelines[54]. The system, made up of three conservation laws, is a drift-flux type model and is closed by two thermodynamic and hydrodynamic models. The complexity of these models makes classical numerical schemes such as Godunov or Roe schemes very difficult to use. Our feeling is that only a "rough" scheme would be able to successfully meet the challenge of nonlinearities.

An essential property of our system is that it possesses fast characteristic speeds (acoustic waves) and slow ones (corresponding to the mass transport phenomenon). From the engineer's standpoint, the crucial aspect is the petroleum transport and not the acoustic. That is why he will never use an explicit scheme, the time step of which is limited by the CFL stability condition : the time required for the simulation would be prohibitive due to the large characteristic speeds.

Inspired by [30], I. Faille and E. Heintze have proposed in [26] a VFRoe-type scheme which is sufficiently rough (diffusive) to handle very stiff industrial cases. The scheme shown in [26] is linearly implicit with respect to the large eigenvalues and explicit with respect to the small eigenvalues. Then

this semi-implicit scheme will combine accuracy on the waves propagating at the small velocities and reduced CPU-time insofar the CFL time step limitation only applies to small eigenvalues.

But this scheme also suffers from a few backdraws. The first one is that the scheme is still CPU-time consuming because it needs to compute numerically the eigenvalues of the Jacobian matrix of the system. The second one is that these eigenvalues are not necessarily real, that is, the system is not always hyperbolic. It is observed in [11] that the system is hyperbolic only if the slip between the phases is not too large.

In [6], the authors have constructed an explicit relaxation scheme by extending Xin and Jin's[69]. The goal was to relax the hydrodynamic and thermodynamic nonlinearities of the system. The genuine nonlinearities are first shown by means of a Lagrangian change of coordinates. Then, these are relaxed. Finally, the equations are brought back to the Eulerian frame. The resulting relaxation system is automatically hyperbolic and has all its fields linearly degenerated. This scheme is less CPU-time consuming than the VFRoe-type one because the most complex (algorithmically speaking) step is the computation of only two relaxation coefficients. Moreover, it has been shown in [6] that one can increase the relaxation coefficients (and therefore the numerical diffusion) in order to satisfy physical properties such as the positivity of the density and, most of all, the maximum principle on the gas mass fraction. As a first attempt to design a fast and rough numerical scheme for two-phase flows, these results were encouraging.

The goal of this paper is to work out a semi-implicit version of the explicit scheme [6] via some mathematically sound extension procedures. In essence, the extension is possible and sound because of the linear degeneracy property of the relaxation system.

The paper is organized as follows. In section 5.1, we introduce the two-phase flow model together with the boundary conditions and the characteristics of this model. In section 5.2, we develop the second order explicit relaxation scheme with the computation of new relaxation coefficients and boundary conditions. In section 5.3, we present the semi-implicit scheme and section 5.4 is devoted to the numerical results.

5.1 Two-phase flow model

5.1.1 Equations

In the flow, the gas (resp. liquid) is characterized by its density $\rho_{\rm G}$ (resp. $\rho_{\rm L}$), its velocity $v_{\rm G}$ (resp. $v_{\rm L}$) and its surface fraction $R_{\rm G} \in [0,1]$ (resp. $R_{\rm L} \in [0,1]$) with the property $R_{\rm L} + R_{\rm G} = 1$. The model is governed by the following system of conservation laws :

$$\left\{ \begin{array}{lll} \partial_t \left(\rho_{\rm L} R_{\rm L}\right) & + \partial_x \left(\rho_{\rm L} R_{\rm L} v_{\rm L}\right) & = 0, \\ \partial_t \left(\rho_{\rm G} R_{\rm G}\right) & + \partial_x \left(\rho_{\rm G} R_{\rm G} v_{\rm G}\right) & = 0, \\ \partial_t \left(\rho_{\rm L} R_{\rm L} v_{\rm L} + \rho_{\rm G} R_{\rm G} v_{\rm G}\right) & + \partial_x \left(\rho_{\rm L} R_{\rm G} v_{\rm L}^2 + \rho_{\rm G} R_{\rm G} v_{\rm G}^2 + p\right) & = S(\mathbf{w}), \end{array} \right. \tag{5.1}$$

for all $x \in \mathbb{R}$ and $t \geq 0$ where the unknown is $\mathbf{w} := (\rho_{\rm L} R_{\rm L},\ \rho_{\rm G} R_{\rm G},\ \rho_{\rm L} R_{\rm L} v_{\rm L} + \rho_{\rm G} R_{\rm G} v_{\rm G})$. Here the source term S includes gravity and wall friction terms which are given functions of the unknown. We will consider a perfect gas and a compressible liquid with the state equations

$$\rho_{\rm G} = p/a_{\rm G}^2, \quad \rho_{\rm L} = \rho_{\rm L}^0 + (p - p^0)/a_{\rm L}^2, \tag{5.2}$$

where p^0 is the atmospheric pressure, $\rho_{\rm L}^0$ is the liquid density for $p = p^0$ and $a_{\rm G}$ (resp. $a_{\rm L}$) is the sound speed in the gas (resp. the liquid). Sometimes, we will use the non-compressible liquid state equation $\rho_{\rm L} = \rho_{\rm L}^0$. The pressure law can be put in the general form $p = p(\mathbf{w}_1,\ \mathbf{w}_2)$ and is smooth function. We consider a general algebraic hydrodynamic law of the type

$$v_{\rm L} - v_{\rm G} = \Phi(\mathbf{w}), \quad \forall\ \mathbf{w} \in (\mathbb{R}^+)^2 \times \mathbb{R}, \tag{5.3}$$

in order to close (5.1). In (5.3), the mapping Φ is assumed to be smooth enough. In practical situations, Φ turns out to be nonlinear in the unknown $\mathbf{w}$ (see [11], [71] for instance).

5.1.2 Boundary and initial conditions

At the inlet of the pipe ($x = 0$), the mass flowrates are given as functions of time, i.e.

$$(\rho_\alpha R_\alpha v_\alpha)(0,\ t) = q_\alpha^0(t),\ t \geq 0,\ \alpha = \mathrm{L}, \mathrm{G},$$

and at the outlet of the pipe ($x = L$), the pressure is a given function of time, i.e.

$$p(L,\ t) = p^L(t),\ t \geq 0.$$

We will treat cases in which the flow is induced only by variations of the boundary conditions : in such experiments, the initial condition is the steady state, computed by the values of the boundary conditions at time $t = 0$.

5.1.3 Characteristics of the model

There is no analytical expression for the physical flux of the considered system, except for very simple hydrodynamic laws. Therefore the eigenvalues of the system (5.1) are not known in full generality. However, in most common situations, i.e., for usual values of $\mathbf{w}$, the system is hyperbolic and has three real eigenvalues $\lambda_1 < \lambda_2 < \lambda_3$ with $\lambda_1 < 0$ and $\lambda_3 > 0$.

The interesting property of the system is that the eigenvalues $\lambda_{1,3}$ correspond to the acoustic waves (or "pressure waves") and propagate at fast speeds thanks to the compressibility of the fluid. The eigenvalue λ_2, which has a variable sign, corresponds to the kinematic waves and propagates at slow speeds with the fluid. These properties imply that the large eigenvalues are 10-100 times bigger than the small eigenvalue, i.e. $|\lambda_{1,3}| \gg |\lambda_2|$.

5.2 Explicit relaxation scheme

Most computational details of this section are given in [6] and only the main results will be reported here.

5.2.1 The relaxation model

Let us consider the total density of the mixing $\rho = \rho_\mathrm{L} R_\mathrm{L} + \rho_\mathrm{G} R_\mathrm{G}$, the total momentum $\rho v = \rho_\mathrm{L} R_\mathrm{L} v_\mathrm{L} + \rho_\mathrm{G} R_\mathrm{G} v_\mathrm{G}$ and ρY where Y denotes the gas mass fraction $Y = \frac{\rho_\mathrm{G} R_\mathrm{G}}{\rho}$ (so that $1 - Y = \frac{\rho_\mathrm{L} R_\mathrm{L}}{\rho}$). The natural phase space associated with such variables then reads :

$$\Omega = \left\{ \mathbf{u} = (\rho,\ \rho v,\ \rho Y) \in \mathbb{R}^3;\ \rho > 0,\ v \in \mathbb{R},\ Y \in [0, 1] \right\}.$$

With some little abuse, both the pressure law p and the hydrodynamic closure Φ will keep their previous notations when expressed in terms of the new variable $\mathbf{u}$. In order to simplify the notations, let us introduce the two following functions of the unknown $\mathbf{u}$:

$$\sigma(\mathbf{u}) = \rho Y(1 - Y)\Phi(\mathbf{u}), \quad P(\mathbf{u}) = p(\mathbf{u}) + \rho Y(1 - Y)\Phi(\mathbf{u})^2. \tag{5.4}$$

Weak solutions of the system (5.1)–(5.3) equivalently obey the following system in conservation form :

$$\left\{ \begin{array}{lcl} \partial_t(\rho) + \partial_x(\rho v) & = & 0, \\ \partial_t(\rho v) + \partial_x(\rho v^2 + P(\mathbf{u})) & = & S(\mathbf{u}), \\ \partial_t(\rho Y) + \partial_x(\rho Y v - \sigma(\mathbf{u})) & = & 0. \end{array} \right. \tag{5.5}$$

We want to relax all the *genuine* non-linearities of the equilibrium system (5.5) which will appear by means of a Lagrangian change of coordinates. Let us set $\tau = 1/\rho$, and define the Lagrangian mass coordinate y by $dy = \rho dx - \rho v dt$. It turns out that expressing the main nonlinearities of the problem in terms of the variables (τ, v, Y) instead of the conservative one leads to simpler calculations. For the sake of simplicity and with some abuse in the notations, nonlinear functions (like the pressure or the hydrodynamic law) will be given the same notation when expressed in both types of variables. The system (5.5) then rewrites :

$$\left\{ \begin{array}{lll} \partial_t \tau & - \partial_y v & = 0, \\ \partial_t v & + \partial_y P(\mathbf{u}) & = S(\mathbf{u}), \\ \partial_t Y & - \partial_y \sigma(\mathbf{u}) & = 0. \end{array} \right. \tag{5.6}$$

Remark 5.2.1 *Let us introduce a new state variable* Π *which is intended to coincide with* P *and let us consider the following* 4×4 *system :*

$$\begin{array}{lll} \partial_t \tau & - \partial_y v & = 0, \\ \partial_t v & + \partial_y \Pi & = S(\mathbf{u}), \\ \partial_t \Pi & + a^2 \partial_y v & = \lambda(P(\mathbf{u}) - \Pi), \\ \partial_t Y & - \partial_y \sigma(\mathbf{u}) & = 0. \end{array} \tag{5.7}$$

This system is hyperbolic and its eigenvalues are $(0, \ \pm a, \ -\sigma_Y)$*. Therefore, on the one hand, the relaxation of the equation* $\partial_t v + \partial_y P(\mathbf{u}) = 0$ *can be seen as a way to enforce the hyperbolicity of the system and to ensure the positivity of the density, as we will see later. On the other hand, it appears that the equation* $\partial_t Y - \partial_y \sigma(\mathbf{u}) = 0$ *is non-linear. The relaxation of this equation can therefore be seen as a way in order to enforce the physical property* $Y \in [0, 1]$*, as we will see later.*

We introduce two new state variables Σ and Π which are intended to coincide respectively with $\sigma(\mathbf{u})$ and $P(\mathbf{u})$ in the limit of the relaxation parameter λ. We propose as a relaxation model the following system :

$$\left\{ \begin{array}{lll} \partial_t \tau & - \partial_y v & = 0, \\ \partial_t v & + \partial_y \Pi & = S(\mathbf{u}), \\ \partial_t \Pi & + a^2 \partial_y v & = \lambda(P(\mathbf{u}) - \Pi), \\ \partial_t Y & - \partial_y \Sigma & = 0, \\ \partial_t \Sigma & - b^2 \partial_y Y & = \lambda(\sigma(\mathbf{u}) - \Sigma). \end{array} \right. \tag{5.8}$$

where a and b are two real positive parameters that we call "relaxation coefficients". We then return back in Eulerian coordinates, where the relaxation system takes the form :

$$\left\{ \begin{array}{lll} \partial_t \rho & + \partial_x (\rho v) & = 0, \\ \partial_t (\rho v) & + \partial_x (\rho v^2 + \Pi) & = S(\mathbf{u}), \\ \partial_t (\rho \Pi) & + \partial_x (\rho \Pi v + a^2 v) & = \lambda \rho (P(\mathbf{u}) - \Pi), \\ \partial_t (\rho Y) & + \partial_x (\rho Y v - \Sigma) & = 0, \\ \partial_t (\rho \Sigma) & + \partial_x (\rho \Sigma v - b^2 Y) & = \lambda \rho (\sigma(\mathbf{u}) - \Sigma). \end{array} \right. \tag{5.9}$$

The above relaxation system will be given hereafter the convenient abstract form :

$$\partial_t \mathbf{v} + \partial_x \mathcal{G}(\mathbf{v}) = \lambda \mathcal{R}(\mathbf{v}) + \mathcal{S}(\mathbf{v}), \quad t > 0, \ x \in \mathbb{R}; \tag{5.10}$$

where the flux function $\mathcal{G}$ receive clear definition and

$$\mathcal{R}(\mathbf{v}) = \quad (0, \ 0, \ \lambda \rho \left(P(\mathbf{u}) - \Pi \right), \ 0, \ \lambda \rho \left(\sigma(\mathbf{u}) - \Sigma \right))^T, \tag{5.11}$$

$$\mathcal{S}(\mathbf{v}) = \quad (0, \ S(\mathbf{u}), \ 0, \ 0, \ 0)^T \tag{5.12}$$

The associated admissible state space $\mathcal{V}$ reads

$$\mathcal{V} = \left\{ \mathbf{v} = (\rho,\ \rho v,\ \rho\Pi,\ \rho Y,\ \rho\Sigma)^T \in \mathbb{R}^5; \right. \\ \left. \rho > 0,\ v \in \mathbb{R},\ \Pi \in \mathbb{R},\ Y \in [0,1],\ \Sigma \in \mathbb{R} \right\}. \tag{5.13}$$

The following Lemma has been proven in [6].

Lemma 5.2.2 *Let (a, b) be a pair of strictly positive real numbers For any $\mathbf{v} \in \mathcal{V}$, the first order system with no source term extracted from (5.9) admits five real eigenvalues :*

$$v,\ v \pm a\tau,\ v \pm b\tau,$$

($\tau = 1/\rho$) and five linearly independent corresponding eigenvectors. Consequently, the first order system with no source term extracted from (5.9) is hyperbolic on $\mathcal{V}$. Moreover, each eigenvalue is associated with a linearly degenerate field.

5.2.2 First order explicit scheme

The pipeline is made of I cells, denoted $(M_i)_{i=1,I}$. Let x_i be the center of the cell and Δx its length. We also denote $x_{i+1/2} = (x_i + x_{i+1})/2$ the interface between two cells, $x_{1/2} = 0$ inlet boundary interface and $x_{I+1/2} = L$ the outlet boundary interface. Let $\Delta t^n = t^{n+1} - t^n$ be the time step. Let $\mathbf{u}_i^n \approx \mathbf{u}(x_i,\ t^n)$ be the discrete unknown. The numerical scheme is based on the following splitting method.

1. Relaxation. We take $\lambda = \infty$ and solve the ODE system $\partial_t \mathbf{v} = \lambda \mathcal{R}(\mathbf{v})$ by projecting the variables on the equilibrium variety. At the beginning of the time step, we compute $\mathbf{v}_i^n \approx \mathbf{v}(x_i,\ t^n)$ at equilibrium, i.e.
$$\Pi_i^n := P(\mathbf{u}_i^n), \qquad \Sigma_i^n := \sigma(\mathbf{u}_i^n). \tag{5.14}$$
2. Evolution. We take $\lambda = 0$ and solve the system $\partial_t \mathbf{v} + \partial_x \mathcal{G}(\mathbf{v}) = \mathcal{S}(\mathbf{v})$ on one iteration in order to go to the time $t = t^{n+1}$.

In the "Evolution" step, we consider the system $\partial_t \mathbf{v} + \partial_x \mathcal{G}(\mathbf{v}) = \mathcal{S}(\mathbf{v})$ that we approximate by the following finite volume scheme :

$$\frac{\mathbf{v}_i^{n+1} - \mathbf{v}_i^n}{\Delta t^n} + \frac{\mathbf{H}_{i+1/2}^{n+1/2} - \mathbf{H}_{i-1/2}^{n+1/2}}{\Delta x} = \mathcal{S}(\mathbf{v}_i^n) \tag{5.15}$$

with $\mathbf{H}_{i+1/2}^{n+1/2}$ the numerical flux based on a Godunov scheme. We denote $\mathbf{v_L} = \mathbf{v}_i^n$ and $\mathbf{v_R} = \mathbf{v}_{i+1}^n$ the left and right states of the Riemann Problem and $\mathbf{v}^\star(\mathbf{v_L},\ \mathbf{v_R})$ the value of the solution of this R.P. at $x = x_{i+1/2}$. The Godunov numerical flux is

$$\mathbf{H}_{i+1/2}^{n+1/2} = \mathbf{H}^{Godunov}(\mathbf{v_L},\ \mathbf{v_R}) = \mathcal{G}(\mathbf{v}^\star(\mathbf{v_L},\ \mathbf{v_R})). \tag{5.16}$$

The explicit computations for $\mathbf{v}^\star$ are given in proposition (5.2.3) at the end of this section. The proposition will not be proven here, since it is done in [6] but is just shown for consistency.

In the following proposition, we denote $\overline{\varphi} = (\varphi_\mathbf{L} + \varphi_\mathbf{R})/2$ the average and $\langle\varphi\rangle = (\varphi_\mathbf{L} - \varphi_\mathbf{R})/2$ the mid-jump of the the two states $\mathbf{v_L}$ and $\mathbf{v_R}$ whatever the quantity φ.

Proposition 5.2.3 *We consider the Riemann problem for the relaxation system (5.9) with $\lambda = 0$ and no source terms and the initial data*

$$\mathbf{v}(x,\ 0) = \begin{cases} \mathbf{v_L} & \text{if } x < 0, \\ \mathbf{v_R} & \text{if } x > 0. \end{cases} \tag{5.17}$$

The Riemann solution is made of six constant states separated by five contact discontinuities

$$\mathbf{v}(x,t) = \begin{cases} \mathbf{v_L} = \mathbf{v}_0 & \text{if } \frac{x}{t} < \mu_1, \\ \mathbf{v}_j & \text{if } \mu_j < \frac{x}{t} < \mu_{j+1}, \quad 1 \le j \le 4 \\ \mathbf{v_R} = \mathbf{v}_5 & \text{if } \frac{x}{t} > \mu_5, \end{cases} \tag{5.18}$$

Let us set

$$\begin{array}{rclcrcl} \tau^\star_{\mathbf{L}} & = & \tau_{\mathbf{L}} - \frac{\langle v\rangle}{a} + \frac{\langle \Pi\rangle}{a^2}, & & \tau^\star_{\mathbf{R}} & = & \tau_{\mathbf{R}} - \frac{\langle v\rangle}{a} - \frac{\langle \Pi\rangle}{a^2}, \\ v^\star & = & \overline{v} + \frac{\langle \Pi\rangle}{a}, & & \Pi^\star & = & \overline{\Pi} + a\,\langle v\rangle\,, \\ Y^\star & = & \overline{Y} - \frac{\langle \Sigma\rangle}{b}, & & \Sigma^\star & = & \overline{\Sigma} - b\,\langle Y\rangle\,. \end{array} \tag{5.19}$$

Assume that the parameter a is chosen large enough so that both $\tau^\star_{\mathbf{L}}$ and $\tau^\star_{\mathbf{R}}$ in (5.19) are positive.

If $a > b$ (see remark (5.2.7)), the eigenvalues are increasingly ordered as follows

$$\underbrace{v_{\mathbf{L}} - a\tau_{\mathbf{L}}}_{\mu_1(\mathbf{v_L})} \le v^\star - b\tau^\star_{\mathbf{L}} \le v^\star \le v^\star + b\tau^\star_{\mathbf{R}} \le \underbrace{v_{\mathbf{R}} + a\tau_{\mathbf{R}}}_{\mu_5(\mathbf{v_R})} \tag{5.20}$$

where the intermediate states are given by :

$$\mathbf{v}_1 = \begin{pmatrix} \rho^\star_{\mathbf{L}} \\ \rho^\star_{\mathbf{L}} v^\star \\ \rho^\star_{\mathbf{L}} \Pi^\star \\ \rho^\star_{\mathbf{L}} Y_{\mathbf{L}} \\ \rho^\star_{\mathbf{L}} \Sigma_{\mathbf{L}} \end{pmatrix}, \ \mathbf{v}_2 = \begin{pmatrix} \rho^\star_{\mathbf{L}} \\ \rho^\star_{\mathbf{L}} v^\star \\ \rho^\star_{\mathbf{L}} \Pi^\star \\ \rho^\star_{\mathbf{L}} Y^\star \\ \rho^\star_{\mathbf{L}} \Sigma^\star \end{pmatrix}, \ \mathbf{v}_3 = \begin{pmatrix} \rho^\star_{\mathbf{R}} \\ \rho^\star_{\mathbf{R}} v^\star \\ \rho^\star_{\mathbf{R}} \Pi^\star \\ \rho^\star_{\mathbf{R}} Y^\star \\ \rho^\star_{\mathbf{R}} \Sigma^\star \end{pmatrix}, \ \mathbf{v}_4 = \begin{pmatrix} \rho^\star_{\mathbf{R}} \\ \rho^\star_{\mathbf{R}} v^\star \\ \rho^\star_{\mathbf{R}} \Pi^\star \\ \rho^\star_{\mathbf{R}} Y_{\mathbf{R}} \\ \rho^\star_{\mathbf{R}} \Sigma_{\mathbf{R}} \end{pmatrix}.$$

5.2.3 Relaxation coefficients

We present in this section the computation of the relaxation coefficients a and b. Our approach is based on the Chapman-Enskog expansions

$$\Pi = P + \lambda^{-1}\Pi_1 + \mathcal{O}(\lambda^{-2}), \tag{5.21}$$

$$\Sigma = \sigma + \lambda^{-1}\Sigma_1 + \mathcal{O}(\lambda^{-2}). \tag{5.22}$$

The point that is different from [6] in the use of these expansions is the following. We will consider the Lagrangian relaxation system (5.8) as the superposition of two decoupled subsystems : the first in $(\tau,\ v,\ \Pi)$ and the second in $(Y,\ \Sigma)$. Furthermore, in order to really decouple these sub-systems, we will make the hypotheses that the non-linear functions P and σ only depends on the equilibrium variables which appear in their respective sub-systems, i.e. $(\tau,\ v)$ for P and Y for σ.

5.2.3.1 Two stability theorems

Let us consider the first sub-system

$$\begin{cases} \partial_t \tau - \partial_y v = 0, \\ \partial_t v + \partial_y \Pi = 0, \\ \partial_t \Pi + a^2\, \partial_y v = \lambda(P - \Pi). \end{cases} \tag{5.23}$$

Theorem 5.2.4 *Under the hypothesis $P = P(\tau,\ v)$, the first order asymptotic equilibrium system of (5.23) is*

$$\partial_t \mathbf{w}^1 + \Gamma^1(\mathbf{w}^1)\partial_y \mathbf{w}^1 = \lambda^{-1}\partial_y \left[\Delta_a(\mathbf{w}^1)\partial_y \mathbf{w}^1\right], \tag{5.24}$$

with $\mathbf{w}^1 = (\tau, v)^T$ and

$$\Delta_a(\mathbf{w}^1) = \begin{pmatrix} 0 & 0 \\ E & a^2 - A \end{pmatrix}, \quad \begin{array}{ll} E = & -P_v P_\tau, \\ A = & -P_\tau + P_v^2. \end{array} \tag{5.25}$$

Proof of Theorem 5.2.4 Substituting (5.21) in (5.23) and neglecting in the third equation of (5.23) the order one terms gives

$$\left\{ \begin{array}{lll} \partial_t \tau & - \quad \partial_y v & = 0, \\ \partial_t v & + \quad \partial_y P & = -\lambda^{-1}\partial_y \Pi_1, \\ \partial_t P + a^2 & \partial_y v & = -\Pi_1. \end{array} \right. \tag{5.26}$$

In the previous system, the two first equations are going to give us the left-hand side of the quasi-linear form (5.24) and the third equation is going to give us the right hand side. But we must change the time derivative of P in space derivatives. To do this, we begin to use the hypothesis $P = P(\tau,\ v)$ in order to have the identity $\partial_t P = \begin{pmatrix} P_\tau & P_v \end{pmatrix} \partial_t \mathbf{w}^1$. Second, the equilibrium system (5.6) gives $\partial_t \mathbf{w}^1 = \partial_y \begin{pmatrix} v & -P \end{pmatrix}^T$.Third, one can derivate P, using the hypothesis for the second time, which gives

$$\partial_y \begin{pmatrix} v & -P \end{pmatrix}^T = \begin{pmatrix} 0 & 1 \\ -P_\tau & -P_v \end{pmatrix} \partial_y \mathbf{w}^1. \tag{5.27}$$

Finally, the composition of the last three identities gives $-\Pi_1 = \partial_t P + a^2 \partial_y \mathbf{w}^1 = \begin{pmatrix} E & a^2 - A \end{pmatrix} \partial_y \mathbf{w}^1$ which conclude the proof. □

Let us consider the second sub-system

$$\left\{ \begin{array}{lll} \partial_t Y & - \quad \partial_y \Sigma & = 0, \\ \partial_t \Sigma & - b^2 \ \partial_y Y & = \lambda(\sigma - \Sigma). \end{array} \right. \tag{5.28}$$

Theorem 5.2.5 *Under the hypothesis $\sigma = \sigma(Y)$, the first order asymptotic equilibrium system of (5.28) is*

$$\partial_t Y - \partial_y \sigma = \lambda^{-1}\partial_y \left[\Delta_b(Y)\partial_y Y\right] \tag{5.29}$$

with

$$\Delta_b(Y) = b^2 - B, \quad B = \sigma_Y^2. \tag{5.30}$$

Proof of Theorem 5.2.5 Similarly, substituting (5.22) in (5.28) and neglecting in the third equation of (5.28) the order one terms gives

$$\left\{ \begin{array}{lll} \partial_t Y & - \quad \partial_y \sigma & = \lambda^{-1}\partial_y \Sigma_1, \\ \partial_t \sigma & - b^2 \ \partial_y Y & = -\Sigma_1. \end{array} \right. \tag{5.31}$$

The hypothesis and the equilibrium system (5.6) gives easily $\partial_t \sigma = B \partial_y Y$. This implies directly $-\Sigma_1 = (B - b^2)\partial_y Y$ which conclude the proof. □

Corollary 5.2.6 *The matrix $\Delta_a(w)$ has its eigenvalues positive and the coefficient $\Delta_b(Y)$ is positive if and only if $a^2 - A \geq 0$ and $b^2 - B \geq 0$.*

Remark 5.2.7 *Because of the specific values of the functions P and σ, we always have $a > b$. This is in harmony with the fact that a is relaxing pressure waves and b kinematic waves.*

5.2.3.2 Practical computation of the relaxation coefficients

We present in this section the computation of the relaxation coefficients a and b. We consider one local couple $(a_{i+1/2},\ b_{i+1/2})$ on each interface $x_{i+1/2}$ in order to minimize the numerical dissipation. The relaxation coefficients are designed in order to ensure :

1. the stability of the first order asymptotic equilibrium system thanks to the Chapman-Enskog expansion. The previous analysis justifies the following choice :

$$\begin{array}{ll} a^1_{i+1/2} = \sqrt{\max(A(\mathbf{u_L}), A(\mathbf{u_R}))}, & A(\mathbf{u}) = -P_\tau(\mathbf{u}) + P_v^2(\mathbf{u}), \\ b^1_{i+1/2} = \sqrt{\max(B(\mathbf{u_L}), B(\mathbf{u_R}))}, & B(\mathbf{u}) = \sigma_Y^2(\mathbf{u}). \end{array} \tag{5.32}$$

   When $\Phi = 0$, we notice that $B(\mathbf{u}) = 0$ and therefore $b^1_{i+1/2} = 0$. This is not compatible with the relaxation method, that is why we modify the relaxation coefficient b in order to have $b^1_{i+1/2} > 0$.
2. physical properties of the approximate solution (positivity of the density and positivity of the mass fractions). As previously exposed in [6], it is possible to compute the relaxation coefficients a and b in order to satisfy the following two basic physical properties : the positivity of the density and, above all, the maximum principle on the gas mass fraction, i.e., $Y_i^n \in [0, 1]$. This is done by computing $a^2_{i+1/2}$ and $b^2_{i+1/2}$ large enough, which results in a increased, but well-adjusted, amount of numerical dissipation.

Finally, on one interface $x_{i+1/2}$, the relaxation coefficient $a_{i+1/2}$ (resp. $b_{i+1/2}$) is computed from the maximum of $a^1_{i+1/2}$ and $a^2_{i+1/2}$ (resp. $b^1_{i+1/2}$ and $b^2_{i+1/2}$).

Remark 5.2.8 *The previous computations are simpler than those in [6]. The fact is that these computations have been discovered in a pragmatic way, considering a numerical experience (a contact discontinuity) in which the old manner led to over-estimated coefficients $b_{i+1/2}$. The resulting numerical solution were very dissipated and therefore unacceptable. We then compared the relaxation coefficients we had for this system and the relaxation coefficients of a scalar equation and of the p-system and finally made the link with the relaxation coefficient exhibited in this paper.*

5.2.4 Second order in space

The scheme is extended to second-order accuracy in space by using the classical MUSCL (Monotonic Upstream Scheme for Conservation Laws) technique ([32], [45]). Instead of taking a constant approximate solution on each cell, we construct a linear approximation. The limited slopes are those of the "physical variable" (p, Y, v) rather than those of the conservative variable $\mathbf{u}$ [26, 27].

5.2.5 Second order in time

We use the following Runge-Kutta second-order procedure. Let us suppose that we denote $\mathbb{L}$ the explicit operator, which is 2nd-order in space, 1st-order in time so that $\mathbf{u}^{n+1} = \mathbb{L}(\mathbf{u}^n)$. Then the explicit second-order both in space and time is :

$$\mathbf{u}^{(1)} = \mathbb{L}(\mathbf{u}^n), \quad \mathbf{u}^{(2)} = \mathbb{L}(\mathbf{u}^{(1)}), \quad \mathbf{u}^{n+1} = \frac{1}{2}\left(\mathbf{u}^n + \mathbf{u}^{(2)}\right). \tag{5.33}$$

5.2.6 Time step

The time step of the relaxation explicit scheme is limited by the CFL condition

$$\frac{\Delta t^n}{\Delta x} \max_{i=1,I} |V_i^n| \leq \mu \tag{5.34}$$

where $\mu = 0.5$ is the CFL and V_i^n is a characteristic speed given by

$$V_i^n = \max\left(\left| v_{i-1/2}^{\mathbf{R}} + a_{i-1/2}\tau_{i-1/2}^{\mathbf{R}} \right|, \left| v_{i+1/2}^{\mathbf{L}} - a_{i+1/2}\tau_{i+1/2}^{\mathbf{L}} \right| \right). \tag{5.35}$$

This condition enables us to obtain a sequence of Riemann problems located at each cell interface $x_{i+1/2}$ without interactions.

5.2.7 Treatment of boundary conditions

In order to take the boundary conditions into account, we introduce two ghost cells : $\mathbf{u}_0^n$ at the inlet of the pipe and $\mathbf{u}_{I+1}^n$ at the outlet. The computation of these two states must be explicit, due to the specific implementation of the linearly implicit scheme.

It is well known that the number of scalar physical conditions to specify on the boundaries is equal to the number of entering characteristics (see for instance Benzoni-Gavage in [11]). We have already notice that our system is hyperbolic and has three real eigenvalues $\lambda_1 < \lambda_2 < \lambda_3$ with $\lambda_1 < 0$ and $\lambda_3 > 0$. Moreover, *in all situations*, at the inlet, $\lambda_2 \geq 0$. Since our system is of dimension 3, this justifies the two physical conditions (q_{L} and q_{G}) at the inlet and just one physical condition (the pressure) at the outlet.

5.2.7.1 Inlet ($x = 0$)

We compute the state $\mathbf{v}_0^n$ in order to satisfy the five following conditions. First, the relaxation state $\mathbf{v}_0^n$ is at equilibrium which leads to the two identities (5.14). Second, we specify the total mass flowrate (which corresponds to the first component ρv) and the gas mass flowrate (which corresponds to the fourth component $\rho Y v - \Sigma$) which leads to the two identities

$$\mathbf{H}^1(\mathbf{v}_0^n,\ \mathbf{v}_1^n) = q_{\mathrm{L}}^0(t^n) + q_{\mathrm{G}}(t^n), \quad \mathbf{H}^4(\mathbf{v}_0^n,\ \mathbf{v}_1^n) = q_{\mathrm{G}}^0(t^n). \tag{5.36}$$

Third, let us introduce ℓ_1 the left eigenvector corresponding to the first eigenvalue of $\nabla\mathcal{G}(\mathbf{u}_1^n)$. We then specify the characteristic projection

$$\ell_1.\mathbf{v}_0^n = \ell_1.\mathbf{v}_1^n. \tag{5.37}$$

The nonlinear system made up of the 5 equations (5.14), (5.36) and (5.37) is solved by a classical nonlinear solver (for instance Newton's method).

5.2.7.2 Outlet ($x = L$)

We compute the state $\mathbf{v}_{I+1}^n$ in order to satisfy the five following conditions. First, the relaxation state $\mathbf{v}_{I+1}^n$ is at equilibrium which leads to the two identities (5.14). Second, we specify the pressure which leads to the identity

$$p(\mathbf{u}_{I+1}^n) = p^L(t^n). \tag{5.38}$$

Third, we could have chosen, as at the inlet, two characteristic projections based on the left eigenvectors corresponding to the fourth and fifth eigenvalues of $\nabla\mathcal{G}(\mathbf{u}_I^n)$. But the experience (based on numerous numerical experiments) shows that it suffices to write the identities

$$Y_{I+1}^n = Y_I^n, \quad v_{I+1}^n = v_I^n. \tag{5.39}$$

The nonlinear system made up of the 5 equations (5.14), (5.38) and (5.39) is solved exactly, with some easy algebraic computations involving the thermodynamic closure laws.

The no-return condition

On offshore petroleum installations, the mixture in vertical pipes ("risers") is falling in a separator which goal is to separate the liquid and gas phases. That is why we would like to enforce the additional condition : the liquid flowrate on the outlet must remain positive. Note that this condition is independent from the change of sign of whatever eigenvalue. The numerical treatment that we have chosen is therefore the following. After having computed the ghost state $\mathbf{v}_{I+1}^n$ satisfying the previous conditions, we compute the numerical flux on the last interface $\mathbf{H}_{I+1/2} = \mathbf{H}(\mathbf{v}_{I+1}^n,\ \mathbf{v}_{I+1}^n)$. We then modify the first component of the flux by

$$\overline{\mathbf{H}}_{I+1/2}^1 = \begin{cases} \mathbf{H}_{I+1/2}^3 & \text{if} \quad \mathbf{H}_{I+1/2}^1 - \mathbf{H}_{I+1/2}^3 \leq 0, \\ \mathbf{H}_{I+1/2}^1 & \text{otherwise.} \end{cases} \tag{5.40}$$

This type of boundary condition is analyzed in the paper of Gallouët [29] which is based on the one of Vovelle [62].

5.3 Semi-implicit relaxation scheme

5.3.1 First order linearly implicit scheme

5.3.1.1 The linear system

Let us consider the relaxation hyperbolic system made up of 5 conservation laws

$$\partial_t \mathbf{v} + \partial_x \mathcal{G}(\mathbf{v}) = \mathcal{S}(\mathbf{v}). \tag{5.41}$$

In the previous Section, we have constructed an explicit scheme which involved the following update of the approximate solution at time t^{n+1} :

$$\mathbf{v}_i^{n+1} = \mathbf{v}_i^n \qquad -\frac{\Delta t^n}{\Delta x}\left(\mathbf{H}(\mathbf{v}_i^n,\ \mathbf{v}_{i+1}^n) - \mathbf{H}(\mathbf{v}_{i-1}^n,\ \mathbf{v}_i^n)\right) + \Delta t^n\ \mathcal{S}(\mathbf{v}_i^n), \tag{5.42}$$

where the right hand side only contains the approximate solution at time t^n. Such a time discretization implies that the time step is sufficiently small (CFL condition) in order for the scheme to be stable. A classical technique to get rid of this limitation is to use the implicit time discretization

$$\mathbf{v}_i^{n+1} = \mathbf{v}_i^n \qquad -\frac{\Delta t^n}{\Delta x}\left(\mathbf{H}\left(\mathbf{v}_i^{n+1},\ \mathbf{v}_{i+1}^{n+1}\right) - \mathbf{H}\left(\mathbf{v}_{i-1}^{n+1},\ \mathbf{v}_i^{n+1}\right)\right) + \Delta t^n\ \mathcal{S}\left(\mathbf{v}_i^{n+1}\right), \tag{5.43}$$

where the computation of the approximate solution at time t^{n+1} is based on the inversion of a nonlinear problem. This inversion is expensive in terms of CPU time. On the other hand, numerical experiments show that the scheme is stable with just one Newton iteration with a far less restrictive

CFL condition. Therefore, we choose this strategy which gives a *linearly implicit* scheme for which the flux $\mathbf{H}$ and the source term $\mathcal{S}$ are approximated by the first-order Taylor expansions

$$\mathbf{H}\left(\mathbf{v}_i^{n+1},\ \mathbf{v}_{i+1}^{n+1}\right) \approx \mathbf{H}\left(\mathbf{v}_i^{n},\ \mathbf{v}_{i+1}^{n}\right) + \partial_1\mathbf{H}\,\delta\mathbf{v}_i + \partial_2\mathbf{H}\,\delta\mathbf{v}_{i+1}, \tag{5.44}$$

$$\mathcal{S}\left(\mathbf{v}_i^{n+1}\right) \approx \mathcal{S}\left(\mathbf{v}_i^{n}\right) + \nabla\mathcal{S}_i\,\delta\mathbf{v}_i, \tag{5.45}$$

where $\delta\mathbf{v}_i = \mathbf{v}_i^{n+1} - \mathbf{v}_i^n$ and where the partial derivatives of $\mathbf{H}$, which are designated by $\partial_1\mathbf{H}$ and $\partial_2\mathbf{H}$, are evaluated at $(\mathbf{v}_i^n,\ \mathbf{v}_{i+1}^n)$ and the Jacobian matrix $\mathcal{S}$ is evaluated at $\mathbf{v}_i^n$. Let us denote

$$\alpha_i = \frac{\Delta t^n}{\Delta x}\partial_1\mathbf{H}(\mathbf{v}_i^n,\ \mathbf{v}_{i+1}^n) \quad \text{and} \quad \gamma_{i+1} = \frac{\Delta t^n}{\Delta x}\partial_2\mathbf{H}(\mathbf{v}_i^n,\ \mathbf{v}_{i+1}^n) \tag{5.46}$$

the partial derivatives of $\mathbf{H}$. Plugging (5.44) and (5.45) in (5.43), one obtains the numerical scheme

$$\begin{aligned}\mathbf{v}_i^{n+1} = \mathbf{v}_i^n \quad & -\frac{\Delta t^n}{\Delta x}\left(\mathbf{H}(\mathbf{v}_i^n,\ \mathbf{v}_{i+1}^n) - \mathbf{H}(\mathbf{v}_{i-1}^n,\ \mathbf{v}_i^n)\right) + \Delta t^n\ \mathcal{S}(\mathbf{v}_i^n) \\ & - (\alpha_i\delta\mathbf{v}_i + \gamma_{i+1}\delta\mathbf{v}_{i+1}) + (\alpha_{i-1}\delta\mathbf{v}_{i-1} + \gamma_i\delta\mathbf{v}_i) + \Delta t^n\ \nabla\mathcal{S}_i\ \delta\mathbf{v}_i. \end{aligned} \tag{5.47}$$

The first three terms of the right hand side of (5.47) corresponds to the explicit scheme. This is why the linearly implicit scheme is classically splitted into three steps.

1. In the physical step, one computes a "predictor" using the explicit scheme

$$\mathbf{v}_i^\sharp = \mathbf{v}_i^n - \frac{\Delta t^n}{\Delta x}\left(\mathbf{H}(\mathbf{v}_i^n, \mathbf{v}_{i+1}^n) - \mathbf{H}(\mathbf{v}_{i-1}^n, \mathbf{v}_i^n)\right) + \Delta t^n\ \mathcal{S}(\mathbf{v}_i^n). \tag{5.48}$$

2. In the mathematical step, one solves the linear equation in $\delta\mathbf{v}$

$$-\alpha_{i-1}\delta\mathbf{v}_{i-1} + \beta_i\delta\mathbf{v}_i + \gamma_{i+1}\delta\mathbf{v}_{i+1} = \mathbf{v}_i^\sharp - \mathbf{v}_i^n \tag{5.49}$$

   where β_i is the matrix $\beta_i = \mathbb{I} + \alpha_i - \gamma_i - \Delta t^n\ \nabla\mathcal{S}_i$ with $\mathbb{I}$ the 5×5 identity matrix. The mathematical step involves a non-symmetric tridiagonal by bloc matrix which is solved by a classical linear solver.

3. Now we can update the conservative variable of the cell i by

$$\mathbf{v}_i^{n+1} = \mathbf{v}_i^n + \delta\mathbf{v}_i. \tag{5.50}$$

Now, the remaining question is : how to construct the matrices α and γ ? It is easy (see [26]) to compute these matrices from the definition (5.46) when the explicit scheme is a Roe-type scheme. The main objective of the next section is therefore to put the relaxation explicit scheme under Roe's form. After that, we will give the explicit computations of the matrices α and γ for the linearly implicit relaxation scheme.

5.3.1.2 Roe's form of the explicit relaxation scheme

We consider the Riemann problem for the relaxation system (5.9) with $\lambda = 0$, no source terms and the left and right states $\mathbf{v}^\mathbf{L} = \mathbf{v}_0$ and $\mathbf{v}^\mathbf{R} = \mathbf{v}_5$. We denote $(\mathbf{v}_j)_{j=1,4}$ the intermediate states and $(\mu_j)_{j=1,5}$ the eigenvalues defined in proposition (5.2.3). It is interesting to compare the following results with the one obtained by Godlewski and Raviart in [31] (chap.III, Section 3.4) while considering the gas dynamic system and rewriting Godunov's method in terms of a Roe-type linearization. Such a rewriting is based on a shock curve decomposition and is possible when the solution of the Riemann problem is made of shocks and contact discontinuities (which is the case of the relaxation system). Let us notice that the following computations are close in spirit from those that appear in the writing of Roe's method (see for instance [31], chap.III, Section 3.1).

Lemma 5.3.1 *With the previous notations, the difference between two consecutive intermediate states of the Riemann problem can be written as*

$$\mathbf{v}_j - \mathbf{v}_{j-1} = \delta_j r_j, \quad j = 1, 5, \tag{5.51}$$

with δ_j the normalization factors

$$\begin{array}{lll} \delta_1 = \rho^\star_{\mathbf{L}} - \rho_{\mathbf{L}}, & \delta_2 = \rho^\star_{\mathbf{L}}(Y^\star - Y_{\mathbf{L}}), & \delta_3 = \rho^\star_{\mathbf{R}} - \rho^\star_{\mathbf{L}}, \\ \delta_4 = \rho^\star_{\mathbf{R}}(Y_{\mathbf{R}} - Y^\star), & \delta_5 = \rho_{\mathbf{R}} - \rho^\star_{\mathbf{R}}, & \end{array}$$

and $R = (r_j)_{j=1,5}$ the matrix

$$R = \begin{pmatrix} 1 & 0 & 1 & 0 & 1 \\ v_{\mathbf{L}} - a\tau_{\mathbf{L}} & 0 & v^\star & 0 & v_{\mathbf{R}} + a\tau_{\mathbf{R}} \\ \Pi_{\mathbf{L}} + a^2\tau_{\mathbf{L}} & 0 & \Pi^\star & 0 & \Pi_{\mathbf{R}} + a^2\tau_{\mathbf{R}} \\ Y_{\mathbf{L}} & 1 & Y^\star & 1 & Y_{\mathbf{R}} \\ \Sigma_{\mathbf{L}} & b & \Sigma^\star & -b & \Sigma_{\mathbf{R}} \end{pmatrix}. \tag{5.52}$$

With the previous lemma, it is easy to construct Roe's matrix thanks to the forthcoming proposition.

Proposition 5.3.2 *Let A^{Roe} be the matrix defined by $A^{Roe}(\mathbf{v}^{\mathbf{L}}, \mathbf{v}^{\mathbf{R}}) = R\Lambda L$ with $\Lambda = Diag(\mu_j)_{j=1,5}$ made of the eigenvalues (5.20), R defined by (5.52) and $L = R^{-1}$. Then A^{Roe} is a Roe's matrix.*

The right eigenvectors of A^{Roe} are obviously the vectors $(r_j)_{j=1,5}$:

$$A^{Roe} r_j = \mu_j r_j, \quad j = 1, 5. \tag{5.53}$$

Let us notice that for $\mathbf{v}^{\mathbf{L}} \neq \mathbf{v}^{\mathbf{R}}$, the Roe's matrix $A^{Roe}(\mathbf{v}^{\mathbf{L}}, \mathbf{v}^{\mathbf{R}})$ is not the value of the Jacobian of the relaxed flux $\mathcal{G}$ at an "average" state.

We define the absolute value of the Roe's matrix by $|A^{Roe}(\mathbf{v}^{\mathbf{L}}, \mathbf{v}^{\mathbf{R}})| = R|\Lambda|L$. The Roe's matrix allows us to construct the Roe's numerical scheme and to conclude, thanks to the forthcoming theorem.

Theorem 5.3.3 *The numerical flux defined by*

$$\mathbf{H}^{Roe}(\mathbf{v}^{\mathbf{L}}, \mathbf{v}^{\mathbf{R}}) = \frac{1}{2}\left(\mathcal{G}(\mathbf{v}^{\mathbf{L}}) + \mathcal{G}(\mathbf{v}^{\mathbf{R}})\right) - \frac{1}{2}|A^{Roe}(\mathbf{v}^{\mathbf{L}}, \mathbf{v}^{\mathbf{R}})|(\mathbf{v}^{\mathbf{R}} - \mathbf{v}^{\mathbf{L}}) \tag{5.54}$$

satisfies the equality

$$\mathbf{H}^{Roe}(\mathbf{v}^{\mathbf{L}}, \mathbf{v}^{\mathbf{R}}) = \mathbf{H}^{Godunov}(\mathbf{v}^{\mathbf{L}}, \mathbf{v}^{\mathbf{R}}) \tag{5.55}$$

where $\mathbf{H}^{Godunov}$ is defined by (5.16).

Such a scheme can be constructed when all the fields of the relaxation system are linearly degenerated, which is our case, or when the solution of the Riemann problem is only made up of shocks.

Proof of Lemma 5.3.1 The main ideas involved in the following computations are the use of the Rankine-Hugoniot condition and the conservation of a well chosen Riemann invariant. The proof of the lemma is composed of the proof of the 5 equalities (5.51), as each equality requests a specific treatment.

In a first step, we show that $\mathbf{v}_1 - \mathbf{v}_0 = \delta_1 r_1$. By definition,

$$\mathbf{v}_1 - \mathbf{v}_0 = (\rho^\star_\mathbf{L} - \rho_\mathbf{L},\ \rho^\star_\mathbf{L} v^\star - \rho_\mathbf{L} v_\mathbf{L},\ \rho^\star_\mathbf{L}\Pi^\star - \rho_\mathbf{L}\Pi_\mathbf{L}, \\ (\rho^\star_\mathbf{L} - \rho_\mathbf{L})Y_\mathbf{L},\ (\rho^\star_\mathbf{L} - \rho_\mathbf{L})\Sigma_\mathbf{L})^T. \tag{5.56}$$

First, the Rankine-Hugoniot condition applied on the Eulerian equation $\partial_t \rho + \partial_x(\rho v) = 0$ with the 1st discontinuity gives

$$\rho^\star_\mathbf{L} v^\star - \rho_\mathbf{L} v_\mathbf{L} = (v_\mathbf{L} - a\tau_\mathbf{L})(\rho^\star_\mathbf{L} - \rho_\mathbf{L}). \tag{5.57}$$

Second, in Lagrangian coordinates, $\mathcal{I} = \Pi + a^2\tau$ is a Riemann invariant for the characteristic speed 0, i.e. $\partial_t \mathcal{I} = 0$. This is a straitforward consequence of the two Lagrangian conservation laws $\partial_t \tau - \partial_y v = 0$ and $\partial_t \Pi + a^2 \partial_y v = 0$. Back in Eulerian coordinates, $\mathcal{I}$ is a Riemann invariant for the characteristic speed v. A direct application is $\Pi^\star + a^2\tau^\star_\mathbf{L} = \Pi_\mathbf{L} + a^2\tau_\mathbf{L}$ which implies $\rho^\star_\mathbf{L}\left(\Pi^\star + a^2\tau^\star_\mathbf{L}\right) - \rho_\mathbf{L}\left(\Pi_\mathbf{L} + a^2\tau_\mathbf{L}\right) = (\rho^\star_\mathbf{L} - \rho_\mathbf{L})\left(\Pi_\mathbf{L} + a^2\tau_\mathbf{L}\right)$. The expansion of the left hand side of the last equality gives

$$\rho^\star_\mathbf{L}\Pi^\star - \rho_\mathbf{L}\Pi_\mathbf{L} = (\rho^\star_\mathbf{L} - \rho_\mathbf{L})\left(\Pi_\mathbf{L} + a^2\tau_\mathbf{L}\right) \tag{5.58}$$

because $\rho^\star_\mathbf{L} \times (a^2\tau^\star_\mathbf{L}) - \rho_\mathbf{L} \times (a^2\tau_\mathbf{L}) = 0$. Substituting equalities (5.57) and (5.58) in the jump (5.56) and using the definitions of δ_1 and r_1 gives $\mathbf{v}_1 - \mathbf{v}_0 = \delta_1 r_1$.

In a second step, the definition of the intermediate states gives

$$\mathbf{v}_2 - \mathbf{v}_1 = [0,\ ,\ 0,\ 0,\ \rho^\star_\mathbf{L}\left(Y^\star - Y_\mathbf{L}\right),\ \rho^\star_\mathbf{L}\left(\Sigma^\star - \Sigma_\mathbf{L}\right)]^T. \tag{5.59}$$

Here, we use the Lagrangian equation $\partial_t Y - \partial_y \Sigma = 0$. We then apply the Rankine-Hugoniot condition with the 2nd discontinuity, which gives $-(\Sigma^\star - \Sigma_\mathbf{L}) = -b\left(Y^\star - Y_\mathbf{L}\right)$. Multiplying each side by $\rho^\star_\mathbf{L}$, one obtains easily

$$\rho^\star_\mathbf{L}(\Sigma^\star - \Sigma_\mathbf{L}) = b\,\rho^\star_\mathbf{L}(Y^\star - Y_\mathbf{L}) \tag{5.60}$$

Substituting the equality (5.60) in the jump (5.59) and using the definitions of δ_2 and r_2 gives $\mathbf{v}_2 - \mathbf{v}_1 = \delta_2 r_2$.

In a third step, the definitions of δ_3 and r_3 gives directly $\mathbf{v}_3 - \mathbf{v}_2 = \delta_3 r_3$. Similarly, one can prove that $\mathbf{v}_4 - \mathbf{v}_3 = \delta_4 r_4$ and $\mathbf{v}_5 - \mathbf{v}_4 = \delta_5 r_5$ which completes the proof. □

Proof of the Proposition 5.3.2 We must show that the matrix A^{Roe} satisfy the three Roe's conditions. This will be done by using the definition of this matrix and some easy computations, as we are going to see.

1. By definition, the matrix $A^{Roe}(\mathbf{v}^\mathbf{L},\ \mathbf{v}^\mathbf{R})$ is diagonalizable with real eigenvalues $(\mu_j)_{j=1,5}$. Its right (resp. left) eigenvectors are $(r_j)_{j=1,5}$, the columns of R (resp. $(l_j)_{j=1,5}$, the lines of L). The five right eigenvectors form a basis of $\mathbb{R}^5$.
2. An easy but tedious calculation enables us to check that $A^{Roe}(\mathbf{v},\ \mathbf{v}) = \nabla\mathcal{G}(\mathbf{v})$.
3. Let us now prove that $A^{Roe}(\mathbf{v}^\mathbf{L},\ \mathbf{v}^\mathbf{R})(\mathbf{v}^\mathbf{R} - \mathbf{v}^\mathbf{L}) = \mathcal{G}(\mathbf{v}^\mathbf{R}) - \mathcal{G}(\mathbf{v}^\mathbf{L})$. First, one can notice that, by definition (5.51), $\mathbf{v}^\mathbf{L} - \mathbf{v}^\mathbf{R} = \sum_{j=1,5}(\mathbf{v}_j - \mathbf{v}_{j-1}) = \sum_{j=1,5}\delta_j r_j$. It is therefore easy to see that, thanks to (5.53) and (5.51),

$$A^{Roe}(\mathbf{v}^\mathbf{L},\ \mathbf{v}^\mathbf{R})(\mathbf{v}^\mathbf{L} - \mathbf{v}^\mathbf{R}) = \sum_{j=1,5}\delta_j\mu_j r_j = \sum_{j=1,5}\mu_j(\mathbf{v}_j - \mathbf{v}_{j-1}).$$

On the other hand, the Rankine-Hugoniot condition gives the jump through the jth discontinuity :

$$\mathcal{G}(\mathbf{v}_j) - \mathcal{G}(\mathbf{v}_{j-1}) = \mu_j(\mathbf{v}_j - \mathbf{v}_{j-1}), \quad j = 1, \ldots, 5. \tag{5.61}$$

It follows that :

$$A^{Roe}(\mathbf{v^L},\ \mathbf{v^R})(\mathbf{v^L} - \mathbf{v^R}) = \sum_{j=1,5} \mathcal{G}(\mathbf{v}_j) - \mathcal{G}(\mathbf{v}_{j-1}) = \mathcal{G}(\mathbf{v^L}) - \mathcal{G}(\mathbf{v^R}),$$

which is the desired result. □

Proof of the Theorem 5.3.3 We use the two equalities ([32], chap 3, lemma 4.3)

$$\frac{2}{\Delta x}\int_0^{\Delta x/2} \mathbf{v}(x/\Delta t^n)dx = \mathbf{v}_5 - 2\frac{\Delta t^n}{\Delta x}\left(\mathcal{G}(\mathbf{v}_5) - \mathbf{H}(\mathbf{v}_0,\ \mathbf{v}_5)\right), \tag{5.62}$$

$$\frac{2}{\Delta x}\int_{-\Delta x/2}^{0} \mathbf{v}(x/\Delta t^n)dx = \mathbf{v}_0 - 2\frac{\Delta t^n}{\Delta x}\left(\mathbf{H}(\mathbf{v}_0,\ \mathbf{v}_5) - \mathcal{G}(\mathbf{v}_0)\right), \tag{5.63}$$

with Δt^n satisfying the CFL condition (5.34). One denotes $\mu_j^+ = \max(\mu_j, 0)$ and $\mu_j^- = \min(\mu_j, 0)$ for $j = 1, 5$. The main idea of the proof is to compute explicitly the left hand sides of (5.62–5.63) and to obtain two distincts expressions for the Godunov numerical flux. As the CFL condition is satisfied, we are sure that $\mu_5^+\Delta t \leq \frac{\Delta x}{2}$ and $\mu_1^-\Delta t \geq -\frac{\Delta x}{2}$ which justify such computations.

The half-sum of these equalities will give a flux involving the eigenvalues and eigenvectors of the Roe's matrix and that will easily be transform into the Roe's numerical flux (5.54).

We want to compute the left hand side of (5.62) by integrating the solution of the Riemann problem on the first domain $(0, \Delta x/2) \times (0, \Delta t^n)$:

$$\begin{aligned}\int_0^{\Delta x/2} \mathbf{v}(x/\Delta t^n)dx &= \mathbf{v}_0\mu_1^+\Delta t^n + \mathbf{v}_1(\mu_2^+ - \mu_1^+)\Delta t^n + \ldots \\ &\quad + \mathbf{v}_4(\mu_5^+ - \mu_4^+)\Delta t^n + \mathbf{v}_5(\frac{\Delta x}{2} - \mu_5^+\Delta t^n)\end{aligned} \tag{5.64}$$

This gives the following identity :

$$\frac{2}{\Delta x}\int_0^{\Delta x/2} \mathbf{v}(x/\Delta t^n)dx = 2\frac{\Delta t^n}{\Delta x}\sum_{j=1,5}(\mathbf{v}_{j-1} - \mathbf{v}_j)\mu_j^+ + \mathbf{v}_5.$$

By comparison with (5.62), one finds :

$$\mathbf{H}(\mathbf{v}_0,\ \mathbf{v}_5) = \mathcal{G}(\mathbf{v}_5) - \sum_{j=1,5}(\mathbf{v}_j - \mathbf{v}_{j-1})\mu_j^+. \tag{5.65}$$

Similarly, the computation of the left hand side of (5.63) by integrating the solution of the Riemann problem on the second domain $(-\Delta x/2, 0) \times (0, \Delta t^n)$ gives :

$$\mathbf{H}(\mathbf{v}_0, \mathbf{v}_5) = \mathcal{G}(\mathbf{v}_0) + \sum_{j=1,5}(\mathbf{v}_j - \mathbf{v}_{j-1})\mu_j^-. \tag{5.66}$$

The equality $|\mu| = \mu^+ - \mu^-$ combined with the half-sum of (5.65) and (5.66) gives :

$$\mathbf{H}(\mathbf{v}_0, \mathbf{v}_5) = \frac{1}{2}(\mathcal{G}(\mathbf{v}_0) + \mathcal{G}(\mathbf{v}_5)) - \frac{1}{2}\sum_{j=1,5}|\mu_j|(\mathbf{v}_j - \mathbf{v}_{j-1}). \tag{5.67}$$

But we have already noticed that $\mathbf{v}_5 - \mathbf{v}_0 = \sum_{j=1,5} \delta_j r_j$ and therefore :

$$\begin{aligned} |A^{Roe}(\mathbf{v}_0, \mathbf{v}_5)|(\mathbf{v}_5 - \mathbf{v}_0) &= \sum_{j=1,5} \delta_j R|\Lambda|L r_j = \sum_{j=1,5} \delta_j |\mu_j| r_j \\ &= \sum_{j=1,5} |\mu_j|(\mathbf{v}_j - \mathbf{v}_{j-1}). \end{aligned}$$

which yields the equality (5.55). □

5.3.1.3 The first-order linearly implicit relaxation scheme

We can now compute the partial derivatives of the Roe's numerical flux $\mathbf{H}(\mathbf{v}^{\mathbf{L}},\ \mathbf{v}^{\mathbf{R}})$ defined by (5.54). They are obtained by making the hypothesis that Roe's matrix is constant. We directly obtain the approximated matrices α and γ

$$\alpha_i \approx \frac{\Delta t^n}{2\Delta x}\left[\nabla \mathcal{G}(\mathbf{v}^{\mathbf{L}}) + \left|A^{Roe}(\mathbf{v}^{\mathbf{L}},\ \mathbf{v}^{\mathbf{R}})\right|\right], \quad \gamma_{i+1} \approx \frac{\Delta t^n}{2\Delta x}\left[\nabla \mathcal{G}(\mathbf{v}^{\mathbf{R}}) - \left|A^{Roe}(\mathbf{v}^{\mathbf{L}},\ \mathbf{v}^{\mathbf{R}})\right|\right]. \tag{5.68}$$

The first-order linearly implicit relaxation scheme consists, at each time step, in solving the linear system $\mathbb{A}\ \delta\mathbf{v} = b$. The matrix $\mathbb{A}$ is a tridiagonal by block matrix with each block of size 5×5 : the resulting matrix is a band matrix with 9 extra-diagonal terms.

We have already shown the interior lines (5.48–5.49) but we have not described the first and the last lines, which are related to the boundary conditions. For the states $\mathbf{v}_0$ et $\mathbf{v}_{I+1}$, we specify $\delta\mathbf{v}_0 = 0$ and $\delta\mathbf{v}_{I+1} = 0$.

5.3.2 First order semi-implicit relaxation scheme

The relaxation scheme is constructed as to be :
- linearly implicit on the fast waves of speed $v \pm a\tau$ ("pressure waves"),
- explicit on the slow waves of speed v ("kinematic waves") and the associated relaxation waves of speed $v \pm b\tau$.

Accordingly, when one computes the partial derivatives of the numerical flux, only the terms associated with the largest eigenvalues are kept. We take the diagonal matrix $\tilde{\Lambda} = diag(v_{\mathbf{L}} - a\tau_{\mathbf{L}},\ 0,\ 0,\ 0,\ v_{\mathbf{R}} + a\tau_{\mathbf{R}})$ which modifies Roe's matrix by $\tilde{A}^{Roe} = R\tilde{\Lambda}L$ with the same matrices R and L as previously. Like Roe's matrix, the eigenvalues of the Jacobian matrices are modified in the same way by $\tilde{A}^{\mathbf{L},\mathbf{R}} = R^{\mathbf{L},\mathbf{R}}\tilde{\Lambda}^{\mathbf{L},\mathbf{R}}L^{\mathbf{L},\mathbf{R}}$. The matrices α and β are then computed with (5.68) and the previous modified matrices.

5.3.2.1 Time step of the semi-implicit relaxation scheme

At each time step, one computes two auxiliary time steps.

1. The explicit time step is :
$$\Delta t^{Void} = \mu^{Void} \frac{\Delta x}{\max_{i=1,I} |V_i^{Void}|}$$
with $\mu^{Void} = 0.5$ and $|V_i^{Void}| = \max\left(|v^\star|,\ |v^\star - b\tau^\star_{\mathbf{L}}|,\ |v^\star + b\tau^\star_{\mathbf{R}}|\right)$.
2. The linearly implicit time step is
$$\Delta t^{Press} = \mu^{Press} \frac{\Delta x_i}{\max_{i=1,I} |V_i^{Press}|}$$
with $\mu^{Press} = 20$ and $|V_i^{Press}| = \max\left(|v_{\mathbf{L}} - a\tau_{\mathbf{L}}|,\ |v_{\mathbf{L}} + a\tau_{\mathbf{R}}|\right)$.

The final time step is $\Delta t^n = \min\left(\Delta t^{Void}, \Delta t^{Press}\right)$. The CFL number $\mu^{Press} = 20$, experimentally determined, turns out to be a good compromise between a small CPU-time and an acceptable amount of smearing out for the numerical solution.

5.3.2.2 Implicit projection

We follow the ideas of Chalons [15]. The use of a linearly implicit scheme implies that the projection step is giving steady states that are not accurate. The solution is to link the evolutions of the relaxed variables associated with an implicit field to the evolutions of the equilibrium variables. In our case, the only relaxed variable associated with an implicit field is $\rho\Pi$: the relaxation variable $\rho\Sigma$ is associated with the eigenvalues $v \pm b\tau$ which are explicit. We therefore write the implicit projection equation :

$$\delta(\rho\Pi)_i = \left(\frac{\partial \mathcal{I}}{\partial \rho}\right)_i^n \delta\rho_i + \left(\frac{\partial \mathcal{I}}{\partial(\rho Y)}\right)_i^n \delta(\rho Y)_i + \left(\frac{\partial \mathcal{I}}{\partial(\rho v)}\right)_i^n \delta(\rho v)_i,$$

with $\mathcal{I}(\mathbf{u}) = \rho P(\mathbf{u})$. The partial derivatives of $\mathcal{I}$ are computed on $\mathbf{u}_i^n$. The previous identity gives an equation that replaces the 5th line of (5.49), i.e., modifies the linear system to be solved in the mathematical step. It enables us to reduce the size of each block from 5×5 to 4×4 and therefore reduce the size of the global linear system.

Numerical experiments shows that not only the steady solutions are more accurate (as already shown in [15]), but even transient solutions are more accurate.

Remark 5.3.4 *The semi-implicit scheme with the implicit projection enables us to use non-constant relaxation coefficients $(a_{i+1/2}, b_{i+1/2})$, as in the explicit scheme. We would like to mention the following link between the implicit projection and the relaxation coefficients.*

1. *The relaxation coefficients associated with linearly implicit fields without the implicit projection must be taken constants (and equal to the maximum over the interfaces).*
2. *The relaxation coefficients associated with linearly implicit fields with an implicit projection can be taken non-constants.*
3. *The relaxation coefficients associated with explicit fields can be taken non-constant.*

These facts are based on numerical experiments : there is no theoretical argument yet to support these facts.

5.3.3 Second order semi-implicit scheme

The slope limiters used to build the second order explicit scheme leads to a non differentiable expression. That is why we choose a simplified version in which we do not differentiate the nonlinear operator involved in the second order correction. In the physical step, we first compute the second order correction of the states $\mathbf{u_{L,R}}$ and evaluate the numerical flux. In the mathematical step, we solve the first order linear system but the derivatives are computed with the corrected states $\mathbf{u_{L,R}}$.

In order to have a second order in time scheme, we use again the Runge-Kutta 2 procedure. Since the scheme is only semi-implicit, the order 2 in time is only achieved on the explicit waves and the linearly implicit waves are solved with order 1 in time.

5.4 Numerical results

In this Section, we show the numerical results of the semi-implicit relaxation scheme : shock tube test (without Boundary Conditions) and real-life cases (with B.C.). The first two test-cases are

Riemann problems. The length of the domain is 100 meters and the discontinuity between the two initial constant states is located at $x = 50$ m. The last two test-cases are real-life problems in which the solution is driven by the changes of the boundary conditions.

5.4.1 Experiment 1 : no-slip law

Closure laws :
- Thermodynamic : non-compressible liquid with $\rho_{\mathrm{L}}^0 = 1000$ kg/m3
  perfect gas with $a_{\mathrm{G}} = 100$ m/s
- Hydrodynamic : no-slip law : $\Phi = 0$

Source terms : No.
Exact solution : 1-rarefaction wave.
Final time : $T = 0.8$ s.
Length of the pipe : $L = 100$ m with Cell size : $\Delta x = 0.5$ m.
Characteristic speeds : $\lambda_{\mathbf{L}}^- = -40.12$ m/s and $\lambda_{\mathbf{R}}^- = -15.77$ m/s.
Left and right states :

$$(\rho, Y, v)_{\mathbf{L}} = (500,\ 0.2,\ 34.4233)\,, \quad (\rho, Y, v)_{\mathbf{R}} = (400,\ 0.2,\ 50)$$

FIG. 5.1 – Detail of experiment 1, no-slip law

The details of this test-case are shown in figure (5.1) and the results are displayed in figure (5.2). We see that the second-order correction leads to a more accurate scheme.

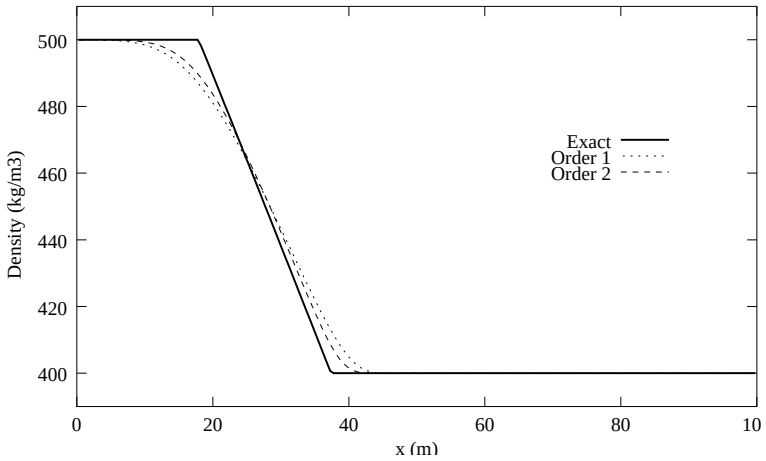

FIG. 5.2 – Numerical results of experiment 1, no-slip law.

5.4.2 Experiment 2 : Zuber-Findlay law

The details of this test-case are shown in figure (5.3) and the results are displayed in figure (5.4). We used the VFRoe-TACITE scheme described in [26] with the same CFL numbers. The two schemes are semi-implicit second-order schemes. The numerical results exhibit a good agreement between the two schemes.

Extracted from : [26]
Closure laws :
- Thermodynamic : non-compressible liquid with $\rho_{\mathrm{L}}^0 = 1000$ kg/m3
  perfect gas with $a_{\mathrm{G}} = 300$ m/s
- Hydrodynamic : Zuber-Findlay law[71] : $\Phi = \frac{(c_0-1)v+c_1}{c_0[XR_{\mathrm{G}}-YR_{\mathrm{L}}]-X}$
  $c_0 = 1.07$, $c_1 = 0.2162$ m/s.

Source terms : No.
Exact solution : . 1-Shock, 2 Contact discontinuity, 3-Shock
Final time : $T = 0.5$ s.
Length of the pipe : $L = 100$ m with Cell size : $\Delta x = 0.5$ m.
Characteristic speeds : $\sigma^- = -40.03$ m/s, $\sigma^0 = 10$ m/s and $\sigma^+ = 67.24$ m/s.
Left and right states :

$$(\rho, Y, v)_{\mathbf{L}} = (453.19,\ 0.00705,\ 24.80)\,, \quad (\rho, Y, v)_{\mathbf{R}} = (454.19,\ 0.0108,\ 1.746)$$

FIG. 5.3 – Detail of experiment 2, Zuber-Findlay law

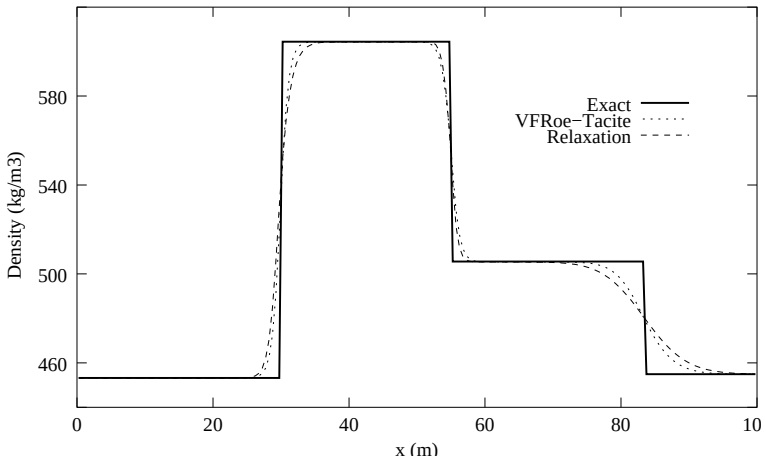

FIG. 5.4 – Numerical results of experiment 2, Zuber-Findlay law.

Extracted from : [53], [26]
Geometry of the pipe and discretization :
- Length : 10000 m, horizontal
- Diameter : 0.146 m
- Cell size : 200 m

Closure laws :
- Thermodynamic : compressible liquid, perfect gas
- Hydrodynamic : no-slip law

Source terms : Friction.
Boundary and initial conditions :
- Stabilization period : 3000 s
- Transient period : 1 s
- Inlet condition on gas flowrate : 0.2 to 0.4 kg/s
- Inlet condition on liquid flowrate : 20 kg/s
- Outlet condition on pressure : 10^6 Pa

FIG. 5.5 – Detail of experiment 3, no-slip law with boundary conditions

5.4.3 Experiment 3 : no-slip law

The details of this test-case are shown in figure (5.5) and the results are given in figures (5.6–5.7). This is the simplest real-life problem we can imagine : we just double the inlet gas flowrate. There is no one-phase states. The numerical results show a good agreement between the two schemes.

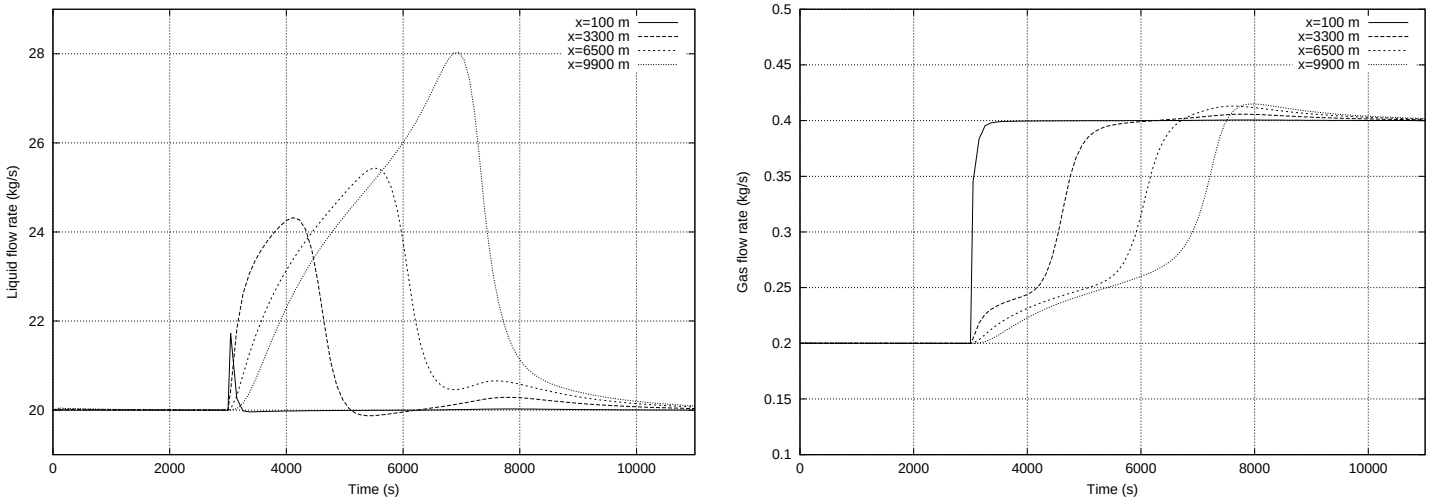

FIG. 5.6 – Experiment 3, TACITE results

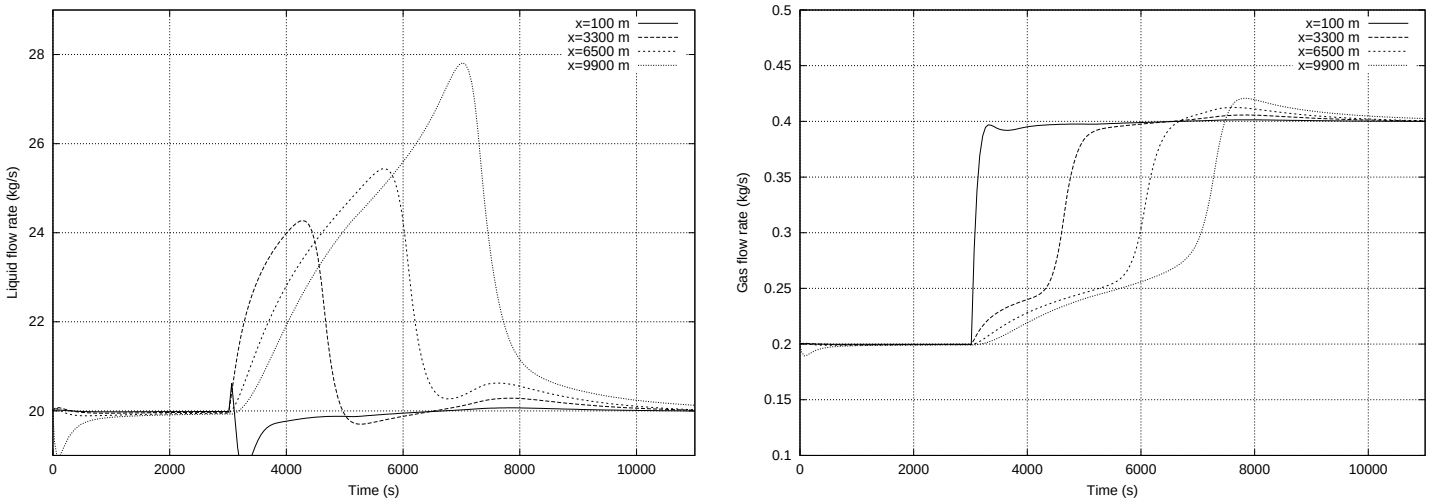

FIG. 5.7 – Experiment 3, relaxation results

5.4.4 Experiment 4 : Zuber-Findlay-like law

The details of this test-case are shown in figure (5.8) and the results are given in figures (5.9).

In this test-case[26], the inlet gas flow rate is decreased from 0.114 to 0 kg/s. As the mass flowrates are small, the decrease in the inlet gas mass flow rate gives rise to negative oil velocities in the upper part of the pipeline. Therefore, a void fraction between a "single-phase gas" state and a "two-phase" state propagates from the outlet down the pipe. Simultaneously, the change in the inlet gas mass flowrates induces another void fraction front which propagates from the inlet up the pipe. These two fronts meet around $x = 47$ m at time $t = 260$ s to form a unique discontinuity wave

Extracted from : [26]
Geometry of the pipe and discretization :
- Length : 80 m, **vertical**
- Diameter : 0.146 m
- Cell size : 1.6 m

Closure laws :
- Thermodynamic : compressible liquid, perfect gas
- Hydrodynamic : like Zuber-Findlay

Source terms : Friction+ Gravity.
Boundary and initial conditions :
- Stabilization period : 10 s
- Transient period : 100 s
- Inlet condition on gas flowrate : 0.114 to 0. kg/s
- Inlet condition on liquid flowrate : 1.628 kg/s
- Outlet condition on pressure : 10^6 Pa

FIG. 5.8 – Detail of experiment 4, Zuber-Findlay-like law with boundary conditions

which propagates towards the outlet. At time $t = 200$ s, this discontinuity wave reaches the outlet and the pipe turns to a single-phase liquid steady state.

This test-case is quite stiff. During the simulation, the scheme must handle two-phase states, liquid state and gas state. Moreover, the discontinuity propagating at the end on the simulation is between two one-phase states. The classical VFRoe scheme is not enough rough in order to handle this case and that is why the authors of [26] introduced more numerical diffusion in their VFRoe-TACITE scheme. The numerical results show a good agreement between the two schemes.

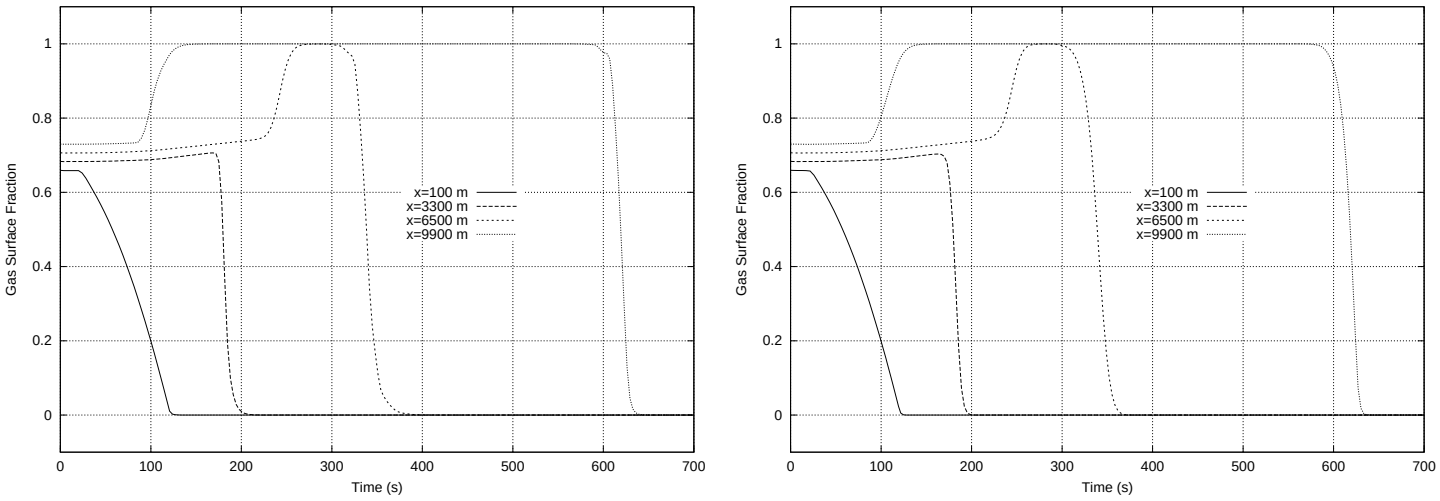

FIG. 5.9 – Experiment 4, gas surface fraction. Left : TACITE results, Right : relaxation.

Conclusion

We have presented a second order semi-implicit relaxation scheme. The main difficulty was to express the relaxation Godunov scheme in Roe's form, that is to say, to compute Roe's matrix. The semi-implicit relaxation scheme is then explicit for the slow waves and linearly implicit for the

fast waves and enable us to reduce the CPU time as well as to be more accurate on slow waves. Numerical experiments show a good agreement with the exact solution on shock tube tests and with a VFRoe-type scheme on more realistic problems.

The main open issue is the extension of this scheme to the compositional flows which have a very important role in petroleum industry. The energy equation should also be investigated in order to take care of thermal effects. A theoretical effort could be made in order to explore the link between the relaxation coefficients and the implicit projection. Another effort could be made in developing rough boundary conditions : the explicit relaxation only ensures the physical properties inside the domain and not at the boundaries.

Acknowledgments

The authors wish to thank I. Faille and F. Willien for the numerous helpful discussions we had.